Dissecting an ancient stress resistance trait syndrome in the compost yeast *Kluyveromyces marxianus*

Kaylee E. Christensen*[,1], Abel Duarte*[,1], Zhenzhen Ma[1,2], Judith L. Edwards[1], Rachel B. Brem[#,1]

[1]Department of Plant and Microbial Biology, University of California, Berkeley, Berkeley, CA, 94720

[2]Current address: Department of Biology, Stanford University, Stanford, CA, 94305

*These authors contributed equally to this work

[#]To whom correspondence should be addressed (rbrem@berkeley.edu)

Abstract

In the search to understand how evolution builds new traits, ancient events are often the hardest to dissect. Species-unique traits pose a particular challenge for geneticists—cases in which a character arose long ago and, in the modern day, is conserved within a species, distinguishing it from reproductively isolated relatives. In this work, we have developed the budding yeast genus *Kluyveromyces* as a model for mechanistic dissection of trait variation across species boundaries. Phenotypic profiling revealed robust heat and chemical-stress tolerance phenotypes that distinguished the compost yeast *K. marxianus* from the rest of the clade. We used culture-based, transcriptomic, and genetic approaches to characterize the metabolic requirements of the *K. marxianus* trait syndrome. We then generated a population-genomic resource for *K. marxianus* and harnessed it in molecular-evolution analyses, which found hundreds of housekeeping genes with evidence for adaptive protein variation unique to this species. Our data support a model in which, in the distant past, *K. marxianus* underwent a vastly complex remodeling of its proteome to achieve stress resistance. Such a polygenic architecture, involving nucleotide-level allelic variation on a massive scale, is consistent with theoretical models of the mechanisms of long-term adaptation, and suggests principles of broad relevance for interspecies trait genetics.

Introduction

A central goal of evolutionary biology is to understand trait diversity in the natural world. In many cases, a character of ecological or industrial interest defines a given eukaryotic species, distinguishing it from its relatives. Dissecting the underlying mechanisms of any such phenotype across species boundaries poses unique technical challenges. As a consequence, against a backdrop of landmark case studies of deep trait divergences in many eukaryotic systems[1–3], principles remain at a premium. What kinds of phenotypes tend to fix in species as they split from one another, and why? How complex is the genetics and what are the causal genes and variants? Addressing these questions requires detailed insights into the physiology of ancient traits and their mechanisms.

Single-celled fungi can serve as a powerful model for evolutionary genetics. *Kluyveromyces,* a genus of budding yeasts, are well-suited to this paradigm given their ~25-million-year divergence[4] and wide-ranging ecology. Microbial sampling studies have isolated *Kluyveromyces* species from a range of terrestrial and aquatic environments, though the genus is best known for its role in food and beverage fermentations[5]. Some *Kluyveromyces* lineages may well have adapted to unique niches long before domestication; to date, few clues to such evolutionary events have emerged[6] (although see the elegant dissection of lactases in dairy-associated *K. marxianus* and *K. lactis*[7]). A deep observational literature has focused on the growth of *K. marxianus* at temperatures exceeding 45°C, motivated by its relevance for the bioproduction industry[8–15]. But the evolution of this thermotolerance trait in *Kluyveromyces*—when, how, and why it arose—remain poorly understood.

We set out to use a comparative approach across *Kluyveromyces* species to investigate the evolution of thermotolerance in this genus. We found that resistance to a range of abiotic stresses, including heat, distinguished *K. marxianus* from the rest of the species of its clade. We used these results as a jumping-off point for the pursuit of the cellular and genetic basis of the *K. marxianus* phenotypic syndrome, and of molecular evolution along the *K. marxianus* lineage.

Results

K. marxianus exhibits a stress resistance syndrome unique in its genus

With the ultimate goal of understanding the evolutionary origin of thermotolerance in *Kluyveromyces*, we first sought to survey stress resistance traits across the genus. We profiled the growth in liquid culture of four species associated with terrestrial habitats (*K. marxianus, K. lactis, K. wickerhamii*, and *K. dobzhanskii*) and three marine species (*K. aestuarii*, *K. siamensis*, and *K. nonfermentans*) (Table S1) in a panel of media conditions (Figure 1). At 42°C, *K. marxianus* exhibited a qualitative growth advantage over its relatives, to an extent far beyond the pattern in a permissive control condition (28°C; Figure 1B). Based on previous population studies of *K. marxianus*[15], we expected that its thermotolerance might be part of a broader, species-unique syndrome of stress resistance. Consistent with this notion, in ethanol, caffeine, and the DNA damage agent methyl methanesulfonate (MMS), *K. marxianus* likewise outperformed the other species of the genus (Figure 1B). Our profiling also identified other conditions in which *K. marxianus* did not stand out with respect to growth (Figure S1). We conclude that *K. marxianus* is unique in the genus for its resistance to some, though not all, abiotic challenges, including high temperature. Given that wild *K. marxianus* isolates tend to phenocopy each other in stress (ref.[15] and Figure S2), we infer that the thermotolerance and chemical stress resistance phenotypes likely arose early in the history of this species, though after its divergence from the rest of the terrestrial *Kluyveromyces* clade.

For many microbes, when cells face nutrient exhaustion, they shut down exponential (log-phase) growth and enter a quiescent, extra-durable state called stationary phase. The difference between *K. marxianus* and its relatives in stress resistance that we had noted in actively dividing cells (Figure 1) might also manifest in the stationary state or, alternatively, its mechanism could be tied to cell growth. To distinguish between these possibilities, we used an experimental design in which we inoculated a given liquid culture into rich medium; incubated for growth at the permissive temperature until nutrient exhaustion; and subjected this stationary-phase culture to a short heat shock. We then tested the extent of cell death during the shock, by assaying the ability of the culture to seed colonies that would grow at the permissive temperature after plating on solid medium (Figure 2A). Results revealed only modest differences between species in heat shock resistance in this stationary-phase heat treatment paradigm, with no particular advantage for *K. marxianus* (Figure 2B). By contrast, when we treated log-phase cultures with heat shock, *K. marxianus* exhibited much higher viability than did the other species of the genus (Figure 2C), paralleling its advantage during chronic high-temperature exposure (Figure 1B). We conclude that for high temperature, the *K. marxianus* advantage only manifests when cells are actively dividing, and that cell death, rather than slow

or arrested growth, mediates the defects of the rest of the genus. The resistance character of *K. marxianus* can thus be seen as a lineage-unique gain of mechanisms that protect cells of this species from lethal failures of the proliferation program under stress.

Major transcriptional remodeling by *K. lactis*, but not *K. marxianus*, in stress

To learn more about the state of *Kluyveromyces* cells under stress, we turned to an expression profiling approach, for which we chose *K. lactis* as a model stress-sensitive species for comparison against *K. marxianus* (Figure 1). We surveyed the transcriptomes of haploid *K. marxianus* (strain Km31, a sugar cane bagasse isolate[16]) and *K. lactis* (lab strain yLB72[17]), in treatments where we had observed divergent growth phenotypes—high temperature, caffeine, MMS, and ethanol—and in a 28°C control (Table S2). In principal component analyses, the strongest contributor to variation across the data set was a program of housekeeping genes expressed more highly in *K. lactis* than *K. marxianus* in all conditions, including controls (Figure 3A, Figure S4A, and Table S2). Also salient on a global scale was a suite of genes that *K. lactis* turned up and down depending on treatment; the *K. marxianus* transcriptome was much less volatile (Figure 3A, Figure S4A, and Table S2).

For a more fine-grained analysis, we tested Gene Ontology groups for coherent, stress-evoked expression change (Table S3). The results revealed housekeeping gene groups induced in stress by *K. lactis*, including ribosomal RNA processing and protein folding (Figure 3B, Figure S4B, and Table S3). Additionally, in a few cases, regulons in *K. lactis* and *K. marxianus* paralleled each other, notably repression of glycolysis and induction of the electron transport chain in some stresses (Figure 3C and Figure S4C). Taken together, however, our transcriptional analyses established programs of elevated expression by *K. lactis*—in stress and in untreated controls—as its major regulatory distinction from *K. marxianus*. Such a pattern would be expected if *K. lactis* underwent more functional failures during growth in our panel of conditions, setting off compensatory expression responses downstream.

The role of respiration in stress is not unique to *K. marxianus*

Growth at high temperature by *K. marxianus* depends in part on respiration[9–12,14]. Given this, and the regulatory changes in carbon metabolism that we had seen in both this species and *K. lactis* under stress (Figure 3A and Figure S4D), we explored the importance of respiration in cell growth across species and treatments. We first assayed viability in our panel of stresses in *K. marxianus* and *K. lactis* under hypoxia. *K. marxianus* exhibited a partial loss of viability by *K. marxianus* in each stress when oxygen was limiting (Figure 4A). A similar effect was detectable for *K. lactis*: even against the backdrop of its weak stress resistance in normoxia, the reduction of oxygen further eroded viability in our focal treatments (Figure 4B). To complement these results with a genetic approach, we tested a *K. marxianus* strain harboring a deletion of the cytochrome oxidase gene *COX15* (ref. [10]) and found a consistent, quantitative reduction in stress resistance relative to wild-type (Figure 4C). We conclude that *K. marxianus* and *K. lactis* both perform at their best when respiring, and that this dependence represents a commonality between the species, likely acting upstream of the mechanisms of their trait divergence.

Widespread evidence for positive selection along the *K. marxianus* lineage

The ecological driving forces for unique traits in *K. marxianus* are unknown, though sampling studies have found this species at high prevalence in high-temperature agricultural and domestic compost[18–20]. We reasoned that some phenotypes unique to *K. marxianus* could have evolved as a product of adaptation to high-temperature or other niches, and that at relevant loci, we could detect evidence for positive selection from sequence data. Toward this end, we first took a phylogenetic approach. We sought to evaluate whether and where *K. marxianus* might harbor unique protein-coding alleles relative to the rest of the *Kluyveromyces* genus, which would have arisen under selection and could underlie phenotypic divergence. For each gene in turn, we aligned orthologs from reference genomes for six species (*K. marxianus, K. lactis, K. wickerhamii*, *K. dobzhanskii*, *K. aestuarii*, and *K. nonfermentans*; Figure 1A). To the alignment we then fit a model specifying positive selection along the *K. marxianus* lineage for some codons, with all other codons and branches evolving under selective constraint, using the branch-site tool in the PAML package[21]. This model was justified, over and above a null model with no selection, for a remarkable 525 genes, with many genes functionally involved in DNA transcription and repair, transmembrane transport, and redox processes (Figure 5A, Figure 5C, and Table S4). By contrast, controls focused on the *K. lactis* branch identified just five genes with signal for positive selection (Figure 5A and Table S4), supporting the inference of a history of particularly avid adaptation in *K. marxianus*.

For most gene hits from our PAML branch-site tests focused on *K. marxianus*, a small number of codons were classified as targets of selection (Figure 5B). We expected that, if the derived alleles at each such site had undergone a selective sweep through *K. marxianus* populations, we could detect it across strains of this species. To test this, we carried out short-read resequencing of the genomes of five wild *K. marxianus* isolates (Table S1) and used the resulting reads alongside our reference genome of the Km31 *K. marxianus* strain as input to a pipeline for SNP calling, pseudogenome construction, and sequence alignment. We then inspected these alignments at each site where the *K. marxianus* allele had arisen under selection according to our analysis of reference genomes with PAML. At 99% of the latter, we detected complete conservation across *K. marxianus* strains (Figure 5C and Table S4). These phylogenetic and resequencing data strongly support a scenario in which derived alleles arose and were maintained by *K. marxianus* under selection, in hundreds of proteins.

To complement our phylogenetic analyses, we next applied population-based molecular-evolution tests using our *K. marxianus* resequencing data and a population-genomic resource for *K. lactis*[22]. We implemented McDonald-Kreitman molecular evolution paradigms[23] to assess evidence for differences in selective pressures between the species on protein sequences, as follows. For each coding region we tabulated sites of non-synonymous and synonymous divergence between *K. marxianus* and *K. lactis*, and likewise for polymorphic variants within the species (Table S5). Using these counts in a McDonald-Kreitman test on a per-gene basis, we identified 11 genes with a significant excess of interspecies amino acid divergence (relative to

polymorphism and for synonymous variation; Figure 5C, Table 1, and Table S5). These results underscored the relatively weak power of the whole-gene McDonald-Kreitman approach in this system, as expected if most positive selection between *K. marxianus* and *K. lactis* involved only a few sites per gene (Figure 5B). However, among the 11 loci that were earmarked by the McDonald-Kreitman test, four had likewise been top-scoring in our phylogenetic analyses (Table 1), representing particularly strong candidate cases of divergence with evolution and phenotypic relevance. Of the McDonald-Kreitman hit genes, four had annotations as plasma membrane transporters or in lipid metabolism, and the remainder had other annotated functions (Table 1).

We also developed a genomic version of the McDonald-Kreitman approach, in which we analyzed non-synonymous and synonymous divergence and polymorphism across cohorts of genes of similar function delineated by Gene Ontology. Most salient from these results were respiration pathways with enrichment for signatures of purifying selection (low ratios of non-synonymous to synonymous polymorphism; Table S6), echoing the dependence on respiration by both *K. marxianus* and *K. lactis* that we had discovered in stress (Figure 3). We also detected signatures of positive selection (enrichment of non-synonymous divergence, normalized for polymorphism and for synonymous variation as the neutrality index) in genes annotated in plasma membrane and transmembrane transporter functions. The latter were partly, but not wholly, attributable to contributions from the top hits of our per-gene McDonald-Kreitman tests (Tables 1 and S6). Thus, genes in these groups were distinguished by a slight but consistent uptick in amino acid variation between *K. marxianus* and *K. lactis*, consistent with the hundreds of amino acid variants across the proteome with a likely history of selection in *K. marxianus* that we had detected phylogenetically (Figures 5A-B). Together, our molecular-evolution results reveal a genomic landscape littered with sites of protein-coding variants unique to *K. marxianus*, strongly suggesting a history of selection on many genes of distinct functions during its 25-million-year history.

Discussion

In the search to understand how and why traits vary between species, the field benefits from powerful genomic inference as well as mechanistic dissection in experimental models[1–3]. In this work, we have established *Kluyveromyces* yeast as a tractable and ecologically relevant platform for the study of species-unique traits. We have characterized a phenotypic syndrome that distinguishes *K. marxianus* from the rest of the genus and have detected evidence for widespread natural selection along this lineage. Our data shed new light on the characters of this species, their physiological mechanisms, and the evolutionary forces that drove their appearance.

Our survey of phenotypes across the *Kluyveromyces* phylogeny enables deep comparative analyses in this system, complementing classic trait compendia[5] and the modern *K. marxianus* literature[8,15,24]. Given the heightened stress resistance by *K. marxianus* relative to the rest of the genus in our profiles, we can date the evolution of the trait syndrome to sometime after *K. marxianus* originated as a species, ~25 million years ago[4]. And given that we and others have seen conservation of resistance traits across *K. marxianus* strains, at least for some focal

stresses[8,15,25], we infer that these unique capacities arose early in *K. marxianus* and persisted during its radiation into modern populations. A model of ecological adaptation by *K. marxianus* would invoke selection to only a subset of stresses relevant to its putative ancestral niche. In many other conditions, *K. marxianus* exhibits no particular advantage and/or resistance is not conserved across strains[8,25].

In pursuit of potential mechanisms of *K. marxianus* stress resistance, we have shown that expression programs are retooled away from fermentation toward respiration, and that limiting oxygen compromises growth, in both *K. marxianus* and *K. lactis* in our focal stresses. Similarly, *Kluyveromyces* species as a rule favor respiration even in the absence of stress[26–29], a life history character that distinguishes the genus from related clades[30]. In light of these general patterns, we do not interpret the reliance on respiration by *K. marxianus* in particular, in heat[8–14] or other stresses, as a direct clue *per se* to the underlying genetic basis of its unique tolerance traits. Respiration may prove to be necessary but not sufficient for derived phenotypes in *K. marxianus*; that is, evolution may have built the traits using new alleles in other gene functions altogether.

Indeed, our molecular-evolution analyses found hundreds of genes, of many housekeeping functions, with evidence for protein variants unique to *K. marxianus* that arose under positive selection. This genome-level signal is consistent with a history of pervasive adaptation by *K. marxianus*, far more so than in its sister lineages. In other systems, signal for selection on such a scale has been reported in the study of major life transitions, *e.g.* the evolution of marine mammals from terrestrial ancestors[31] and snakes from tetrapod ancestors[32], and in analyses of convergent traits in species complexes[1], from tomato[33] to long-lived fishes[34] and eusocial bees[35].

What could the ecological pressures have been on an *K. marxianus* ancestor? Though well-recognized as an industrial dairy yeast[7,36–39], *K. marxianus* was likely domesticated for this purpose fairly recently, as inferred for *K. lactis*[22]. And though *K. marxianus* can be isolated from rotting fruit[40,41], it may not have specialized narrowly to such substrates: a neighboring clade that includes *Saccharomyces cerevisiae* produces more ethanol than do any of the *Kluyveromyces* species[6], suggesting a weaker drive in the latter toward this putative mechanism to kill off microbial competitors in high-sugar environments. Perhaps most compelling among microbial ecology findings is the prevalence of *K. marxianus* in decomposing plant material beside fruit, including leaf litter and pine needles[42], cow dung[19] and industrially processed cocoa beans[43], agave[44], and sugar cane[16,45]. If the ancestral niche for *K. marxianus* included plant substrates of this kind, the yeast could have specialized in rapid metabolism of free sugars, leaving the breakdown of lignocellulosic plant cell wall components to other fungal saprotrophs. Furthermore, in this scenario, we can envision that chemical stress resistance by *K. marxianus* arose in response to plant defense compounds in the decomposing material[46]; metabolites and the capacity to make them can persist in plant tissues for days after abscission or harvest[47,48]. And some evidence for low pH deep in compost piles[49] suggests that this condition could also have shaped *K. marxianus* evolution. In any case, even if we assume an ecological association

with plant sources for ancestral *K. marxianus*, it has come to occupy a broad range of niches, including soil and human and animal material[39,50–52].

In *K. marxianus*, hit loci from our molecular-evolution methods span a much wider range of annotations than the variant cell growth genes mapped in previous studies of *S. cerevisiae* thermotolerance[53–55]. Relative to the latter, it is tempting to speculate that this discrepancy reflects the evolution of resistance to a bigger swath of stresses by *K. marxianus*. That said, our work leaves open the causal link between the derived alleles we have traced in the *K. marxianus* genome and the phenotypes of this species, though phenotyping of *K. marxianus* x *K. lactis* F1 hybrids established that the *K. marxianus* phenotype was partially dominant (Figure S5). If adaptive traits in *K. marxianus* were mediated by hundreds of independent variants, it would conform to the current view of dizzying genetic complexity as the rule rather than the exception for trait variation, across the tree of life[56,57]. In fact, even our large set of loci with signatures of selection could represent an underestimate of the full genetic architecture of *K. marxianus* traits, given the potential of false negatives in our approach as well as the contribution from species-specific genes[58] not analyzed here. But even as they stand, the derived alleles we have discovered in *K. marxianus* represent candidate determinants that would be sufficient to reconstitute *K. marxianus* traits in a stress-sensitive background; as such, they provide an important complement to the few reports focused on genes necessary for thermotolerance in this species[10,13,58].

Assuming dozens or hundreds of species-unique variants ultimately explain the *K. marxianus* trait syndrome, they could have accumulated over a very long time. Current theory[59,60] would posit that, along the *K. marxianus* lineage, a first advantage arose in ecologically relevant stress conditions as a product of selective sweeps in a few major-effect loci, followed later by the accumulation of many more variants with smaller adaptive effects. Dynamics of this kind, assuming they emerge as generally relevant, could unify the current understanding of genetically simple, recent, intraspecies (local) adaptations[61] with that of more ancient traits. Empirical validation of this model, in lower and higher organismal systems, represents an ongoing goal of interspecific genetics.

Methods

1. Strains

Strains used in phenotyping experiments (Figures 1-4, S1,2,4,5) and population analysis (Figure S2, Table 1) are listed in Table S1.

2. Liquid growth phenotyping of wild-type *Kluyveromyces*

Liquid culture experiments in stress and standard-condition controls in Figure 1 used *K. marxianus* Km31; *K. lactis* yLB72; and the strains of *K. dobzhanskii, K. wickerhamii, K. nonfermentans, K. aestuarii*, and *K. siamensis* listed in Table S1. For a given species and condition, we streaked a frozen stock onto yeast peptone dextrose (YPD) agar plates, incubated

for two days at 28°C, picked a single colony, inoculated into 5 mL liquid YPD, and incubated with shaking at 28°C for 16-18 hours. We call this the first pre-culture. We diluted, into fresh liquid YPD, an inoculum of the first pre-culture at the volume required to attain an optical density (OD_{600}) of 0.05 for a total culture volume of 5 mL, and we incubated this second pre-culture with shaking at 28°C for ~7 hours until it reached OD_{600} = 0.2. For unstressed controls in Figure 1, we diluted an inoculum of the second pre-culture into fresh liquid YPD at the volume required to attain OD_{600} = 0.2 for a total culture volume of 5 mL. 150 µL of this experimental culture was transferred to each of 12 wells of a 96-well plate, sealed with a Breathe-Easy membrane (Diversified Biotech), for incubation at 28°C and growth measurements across a 24-hour timecourse in a Tecan M200 PRO plate reader (parameter time point measurement, OD_{595}). For heat stress treatment in Figure 1, setup and growth assays were as above except that incubation of the experimental culture was at 42°C. For chemical stress treatments in Figure 1, setup and growth assays were as above except that for the experimental culture, before transfer to the 96-well plate, ethanol (Koptec) was added to attain a concentration of 6.5% (v/v); caffeine (Sigma-Aldrich) was added to attain 25 mM; or methane methylsulfonate (MMS; Thermo Scientific) was added to attain 0.03% (v/v), and growth timecourses were 48 to 72 hours. For chemical stress treatments and growth measurements in Figures S1 and S2, for a given species and condition, streaking and the first pre-culture were as above. We diluted an inoculum of the first pre-culture into fresh liquid YPD at the volume required to attain OD_{600} = 0.2 for a total culture volume of 5 mL, with 1 M NaCl (Fisher), 3% glycerol (v/v; Fisher), 80 mM $CaCl_2$ (Sigma), 250 mM rapamycin (Research Products International), or 6 mM H_2O_2 (Fisher), followed by incubation and growth measurements in the 96-well format as above.

Experiments in Supplementary Figure 5 used a *ura3-/-* F1 hybrid formed by the mating of *K. marxianus* Km31 and *K. lactis* yLB72. Phenotyping was as Figure 1, except that the first pre-culture had a volume of 10 mL, and each species was inoculated into 8 wells of a 96-well plate for incubation and growth measurements.

3. Assays of cell survival from *K. marxianus* and *K. lactis* stationary and log-phase liquid culture

For survival assays of cells in exponential phase in Figures 2 and S3, for *K. marxianus* Km31 and separately for *K. lactis* yLB72 we streaked a frozen stock onto yeast peptone dextrose (YPD) agar plates, incubated for two days at 28°C, picked a single colony, inoculated into 5 mL liquid YPD, and incubated with shaking at 28°C for 16-18 hours. We diluted, into fresh liquid YPD, an inoculum of this first pre-culture at the volume required to attain OD_{600} = 0.05 for a total culture volume of 5 mL, and we incubated this second pre-culture with shaking at 28°C for ~7 hours until it reached OD_{600} = 0.2. We took this second pre-culture directly into experimental treatment as follows. For unstressed controls, serial dilutions of the culture were spotted onto agar plates and incubated for 2 days at 28°C. For heat shock, 1 mL of the culture was incubated in a heat block at 47°C for 30 minutes and then transferred to ice for 2 minutes, followed by spotting and incubation as above.

For survival assays of cells in stationary phase in Figures 2 and S3, for *K. marxianus* Km31 and separately for *K. lactis* yLB72 we streaked a frozen stock onto yeast peptone dextrose (YPD) agar plates, incubated for two days at 28°C, picked a single colony, inoculated into 5 mL liquid YPD, and incubated with shaking at 28°C for 96 hours. Heat shock and spotting (and unstressed controls) were as above.

4. Transcriptional profiling

4.1. Culture protocol and experimental designs. For a given replicate of RNA-seq of *K. marxianus* Km31 and separately for *K. lactis* yLB72 in unstressed control conditions, we isolated a single colony on solid plates and carried out first and second pre-cultures in liquid YPD at 28°C as in Section 2. For unstressed controls, we diluted an inoculum of the second pre-culture into fresh liquid YPD at the volume required to attain OD_{600} = 0.05 for a total culture volume of 50 mL. This experimental culture was incubated at 28°C with shaking until it reached OD_{600} = 0.4-0.85. From this culture we took a volume corresponding to 2 OD units, pelleted its cells by centrifugation for 5 minutes at 1,500 x g, and resuspended in 1 mL of RNAlater (ThermoFisher) followed by storage at 4°C for up to 48 hours. For RNA-seq of heat-stressed cells, culture, pelleting, and storage were as above except that the experimental culture was incubated at 37°C or 39°C; for RNA-seq of cells under chemical stress, culture, pelleting, and storage were as above except that the experimental culture was done in YPD with 22 mM caffeine, 0.01% MMS, or 3% ethanol. For expression-based reannotation of *K. marxianus* Km31 and *K. lactis* yLB72 (see below), we used the above pipeline for a preliminary expression profiling experiment which we call the training batch: we cultured one biological replicate of Km31 and yLB72 at 37°C and one of Km31 and yLB72 in unstressed control conditions. For comprehensive transcriptional profiling analyses in Figure 3 and Figure S4, we used the above pipeline to generate cell pellets in two production batches. In one batch we grew three biological replicates of Km31 and three of yLB72 in 39°C heat stress, and three unstressed cultures of each species. In another batch we grew three biological replicates of each species in caffeine, three in MMS, and three in ethanol, and three unstressed controls.

4.2. RNA isolation and sequencing. For RNA isolation of a given sample pellet stored in RNAlater (see Section 4.1), we centrifuged for 5 minutes at 1,500 x g, and after decanting of the supernatant, we resuspended the pellet in 200 µL of nuclease-free water followed by addition of 750 µL of BashingBead buffer from the Direct-Zol RNA MicroPrep RNA kit (Zymo Research). We then transferred our 950 µL of suspension into BashingBead tubes, vortexed for 20 minutes, and centrifuged for 5 minutes at 12,000 x g. We took ~600 µL of supernatant from the top layer being careful not to touch the pellet, transferred to a new tube, and mixed with an equal volume of 100% ethanol. This mixture was used as input to the rest of the kit, following the manufacturer's instructions. RNA library preparation and sequencing of ~20M 150 bp paired-end reads per sample was carried out by Novogene, Inc.

4.3. Genome re-annotation and ortholog calls for K. marxianus *and* K. lactis

To generate a reference genome for *K. marxianus* strain Km31, we proceeded as follows. We first used bwa (bio-bwa.sourceforge.net) to map the RNA-seq reads from the *K. marxianus* cultures of the training batch of our transcriptional profiling (see Section 4.1) to a published genome of the DMB1 strain of *K. marxianus*[18]. We then used these mappings, requiring mapping qualities of >20 and mapped lengths >20, to call single-nucleotide polymorphisms with BCFtools[62,63] mpileup with the -I flag to ignore indels, and filtering for exclusion of variants with: a depth of less than 10 reads, or more than 10% of reads with a mapping quality of 0 supporting the variant. For the called polymorphisms, we computationally introduced Km31 alleles into the DMB1 genome sequence with the consensus tool in BCFTools to generate a first-pass pseudogenome for Km31. Next, we used this pseudogenome and the training batch RNA-seq reads as input into transcript assembly with trinity (github.com/trinityrnaseq.trinityrnaseq/wiki) and annotation with PASA (https://sourceforge.net/projects/pasa/), and we took the output as our final annotated genome for *K. marxianus* Km31 (Supplementary Data 1). We generated a reference genome for *K. lactis* strain yLB72 as above, except that we used RNA-seq from the *K. lactis* training batch and the published genome of *K. lactis* strain NRRL Y-1140[64] (Supplementary Data 1). To call orthologous gene pairs between *K. marxianus* Km31 and *K. lactis* yLB72, we used our final annotations from the two species as input into OrthoFinder[65]. We retained all one-to-one orthology calls, *i.e.* cases in which a single annotated gene from *K. marxianus* was called orthologous to a single gene from *K. lactis*. We also sought to valorize cases in which OrthoFinder, with the goal of finding orthologs in species B of a gene $G_{1,A}$ in species A, did not distinguish between *n* candidate orthologous genes $G_{1...n,B}$ from species B. We evaluated each candidate $G_{i,B}$ for synteny: if the next gene up- or downstream of $G_{i,B}$ in the species B genome was called a one-to-one ortholog of the up- or downstream genes of $G_{1,A}$ in the species A genome, we retained this case as a bona fide ortholog pair. Our final set comprised 3578 ortholog pairs between *K. marxianus* Km31 and *K. lactis* yLB72. *Saccharomyces* orthologs were taken from ref. [66].

4.4. Production-batch transcriptional profiling data analysis

For comprehensive transcriptional profiling analyses in Figure 3 and Figure S4, we used our RNA-seq data from cultures of *K. marxianus* Km31 and *K. lactis* yLB72 from production batches (see Section 4.1) as follows. For the RNA-seq reads from a given replicate of a given species (*K. marxianus* or *K. lactis*) and condition (39°C, ethanol, caffeine, MMS, or unstressed control), we mapped to the respective pseudogenome (see Section 4.3) using the TopHat[67] aligner with default parameters, and we used these mappings as input into HTseq[68] to generate raw read counts per gene. For a given species and stress, we used the counts from all replicates from the stress, and the unstressed control from the respective batch, as input into edgeR[69] to generate normalized counts per gene and replicate and a normalized $\log_2$ fold-change between stress and control conditions as an average across replicates. Principal component analysis (PCA) of the RNA-seq data was done using the PCA module of scikit-learn[70]. The edgeR normalized counts for each gene in each treatment were scaled to unit variance with scikit-learn before running the PCA. Principal component weights are listed in Supplementary Table 2.

To identify gene groups in which a given stress treatment evoked significant gene induction or repression relative to the unstressed control, in *K. marxianus* Km31 and separately in *K. lactis* yLB72 (Table S3), we carried out resampling-based enrichment tests as follows. We used assignments of each gene to Gene Ontology terms for *K. lactis* from FungiDB (https://fungidb.org/fungidb/app/record/dataset/NCBITAXON_284590, downloaded January 2022), and we propagated these assignments to orthologous genes in *K. marxianus* from Section 4.3. For a given species and stress, for each Gene Ontology term in turn, for the n genes from the term with expression observations, if $n > 5$ we collated the genes' $\log_2$ fold-changes in expression between stress and the untreated control, each of which was a mean across replicates (from edgeR; see above). We took the mean of these fold-changes across the genes of the term, m_{true}. We then picked n random genes from the genome and tabulated their mean expression fold-change for the respective species and stress, $m_{resample}$. Repeating the latter resampling 1000 times, we calculated an empirical p-value reporting the enrichment of the magnitude of expression fold-change as the percentage of resamples for which ($|m_{resample}| \geq (|m_{true}|$). We used the p-values for all terms tested for the respective species and stress as input into multiple testing correction with the Benjamini-Hochberg method.

5. Assays of cell survival from *K. marxianus* and *K. lactis* anaerobic and aerobic liquid cultures

As *Kluyveromyces* cannot tolerate strictly anaerobic conditions[27,29,71,72], for Figure 4 we used a limited-oxygen experimental paradigm[9] as follows. For *K. marxianus* Km31 and separately for *K. lactis* yLB72, for each treatment we isolated a single colony on solid plates and carried out first and second pre-cultures in liquid YPD at 28°C under aerobic conditions as in Section 2. For unstressed controls in anaerobic conditions, we diluted an inoculum of the second pre-culture into fresh liquid YPD at the volume required to attain $OD_{600} = 0.05$ for a total culture volume of 5 mL. 150 µL of this experimental culture was transferred to each of 12 wells of a 96-well plate, which was placed (with lid) into an AnaeroPouch (ThermoScientific) with a AnaeroPouch - Anaero gas pack. The sealed pouch and plate were incubated for 72 hours at 28°C. Then we collected 30 µL of culture from each well and combined them all into one master culture, 100 µL of which we serially diluted into spots on agar plates, followed by incubation for 2 days at 28°C. Aerobic controls were treated analogously except that the 96-well plate was inoculated without a pouch. Viability assays of chemically stressed cells in anaerobic conditions and aerobic controls were as above except that for the experimental culture, before transfer to the 96-well plate, ethanol, caffeine, or MMS were added as in Section 2. Viability assays of heat-treated cells in anaerobic conditions and aerobic controls were as above except that the sealed pouch and plate were incubated for 24 hours at 39°C.

6. *K. marxianus cox15* mutant generation and liquid growth phenotyping

To knock out *COX15* in the *K. marxianus* Km31 background, we first generated three oligos by PCR: (1) the 1000-bp region from the Km31 genome upstream of the *COX15* coding start; (2) the kanamycin resistance cassette from the genome of a marked version of the haploid *Saccharomyces cerevisiae* strain DBVPG1373 from the Sanger Centre's *Saccharomyces*

Genome Resequencing Project (MATa ura3Δ::KanMx; National Collection of Yeast Cultures); and (3) the 1000-bp region downstream of the *COX15* coding stop. On the 3' end of amplicon 1 was a ~40-bp tail corresponding to the sequence of the first 40 bp of amplicon 2; likewise, on the 5' end of amplicon 3 was a ~40-bp tail corresponding to the last 40 bp of amplicon 2. We stitched the three together via PCR using primers at the extreme 5' and 3' ends of amplicons 1 and 3, and we subjected the stitched-amplicon product to NucleoSpin column cleanup (Takara). We transformed the stitched amplicon into Km31 by electroporation[73] and selected transformants by plating onto agar plates with 200 µg/mL of G418 (Gibco). Sanger sequencing confirmed replacement of the *COX15* coding region by the cassette. For stress phenotyping and unstressed controls of the *cox15* mutant and Km31 wild-type in Figure 4C, protocols were as for the anaerobic assays (see Section 5), except without the use of the anaerobic pouch and heat-treated cells were incubated at 45°C.

7. Molecular-evolution analyses

7.1. Phylogenetic analyses

As input to phylogenetic analyses of one strain for each *Kluyveromyces* species for Figure 5 and Table S4, genomes and annotation were as follows. For *K. marxianus* and *K. lactis* we used the reference genomes and annotations of Km31 and yLB72, respectively, from Section 4.3. For *K. wickerhamii* we used the reference genome and annotation of UCD54-210 from[66]. For the *K. nonfermentans* strain NRRL Y-27343[74], the *K. aestuarii* strain NRRL YB-4510[75], and the *K. dobzhanskii* strain NRRL Y-1974[76] we used YGAP[77] to generate *de novo* annotations from previously generated reference genomes (Supplementary Data 1). We called orthologs across the six species with OrthoFinder[65], and for a given orthogroup we generated protein alignments using MUSCLE[78]. We then used this alignment and its nucleotide sequences as input into PAL2NAL[79] using the -nogap flag to remove gaps to generate a codon alignment.

For each orthogroup in turn, we ran the PAML[21] codeml package run using the branch-site model[80] to evaluate the fit to the sequence data of a model in which regions of the coding sequence are under positive selection for amino acid variation along a focal (foreground) branch and not on any other branch from the tree (the background branches). We used as input to PAML the codon alignment for the orthogroup and the topology of the phylogenetic tree relating the species (see Figure 1A), omitting *K. siamensis*. The calculation proceeded in two steps. First, we fit a null model in which all branches of the tree had the same protein evolutionary rate (PAML codeml run with options verbose = 1, seqtype = 1, clock = 0, model = 2, NSsites = 2, fix_omega = 1, omega = 1), yielding a protein evolutionary rate and log-likelihood of the data under the model. Next, we re-fit using an alternative model in which the branch leading to *K. marxianus* was the foreground (PAML codeml run with options verbose = 1, seqtype = 1, clock = 0, model = 2, NSsites = 2, fix_omega = 0). Outputs were the codon sites assigned to the class with an excess of amino acid changes in *K. marxianus* relative to silent changes, and their posterior probabilities under Bayes Empirical Bayes inference[81]; the codon sites assigned to classes with relaxed and purifying selection, respectively, along the background lineages, and their posterior probabilities; and the log-likelihood of the data under the model. The *p*-value

assessing the improvement in fit to the data of the alternative model relative to the null was calculated from a likelihood ratio test (a χ^2 test on twice the difference of likelihoods with one degree of freedom). *p*-values were corrected for multiple testing by the Benjamini/Hochberg method using the multipletests function from statsmodels[82]. In Figure 5A we tabulated all genes with adjusted $p < 0.05$ from this test that had more than 1% of codon sites assigned to the class with an excess of amino acid changes in *K. marxianus* (proportion in class 2a > 0.01 in codeml). Separately, we repeated the above analyses using the branch leading to *K. lactis* as the foreground. Conservation of sites called significant by PAML using *K. marxianus* as the foreground were calculated with a personal script utilizing Biopython[83] to count the conservation of each site among our sequenced *K. marxianus* strains (Table S1, see Section 7.2). *Saccharomyces* orthologs were taken from ref. [66].

7.2. Resequencing and analysis of K. marxianus *and* K. lactis *population genomes*

For resequencing, we cultured, in 10 mL of liquid YPD, each of five *K. marxianus* strains of non-domesticated provenance beside Km31, and two non-domesticated *K. lactis* strains beside yLB72 (Table S1), and we isolated DNA from each with the Quick-DNA™ Fungal/Bacterial Miniprep Kit (Zymo Research). Genomic DNA sequencing libraries were made and sequenced on an Illumina NovaSeq 6000 by the UC Berkeley Vincent J. Coates Genomic Sequencing Laboratory. We used Minimap2[84] to map the *K. marxianus* reads to our *K. marxianus* Km31 reference genome (see Section 4.3). Separately, we mapped the reads from each of 41 *K. lactis* strains previously sequenced[22], and those from our two sequenced *K. lactis* strains, to our *K. lactis* yLB72 reference genome. For each strain we sorted mappings using the SAMtools fixmate and markdup functions, and we called single-nucleotide polymorphisms and generated a pseudogenome as in Section 4.3, except the variant filtering included only a quality score (QUAL) threshold of above 20. Called variants are provided in Supplementary Data 2. For each pair of orthologous genes between *K. marxianus* and *K. lactis* from section 4.3, we aligned the nucleotide sequences of the coding regions from all strains of the two species using MUSCLE[78]. We then used this alignment and its associated nucleotide sequences as input into PAL2NAL[79] using the -nogap flag to remove gaps to generate a codon alignment.

For Table 1 and Table S5 we carried out per-gene McDonald-Kreitman analyses[23] on the PAL2NAL alignments using the mktest function from the CodonAlignment class from Biopython. *p*-values were corrected for multiple testing by the Benjamini/Hochberg method using the multipletests function from statsmodels[82]. For a given gene, this approach tabulates the rates of non-synonymous polymorphism within species (P_n), synonymous polymorphism (P_s), non-synonymous divergence between species (D_n), and synonymous divergence (D_s), and the neutrality index NI = $(P_n/P_s)/(D_n/D_s)$. Because low counts of amino acid polymorphism can drive significance in the McDonald-Kreitman framework, we developed a filtering scheme in which we tabulated the average *a* and standard deviation σ of P_n/P_s across all genes for which we had sequence data. We only retained for Table 1 and NI genomic analyses those genes with $P_n/P_s > a - 1.5\sigma$.

For genomic analyses of P_n/P_s and D_n/D_s in the McDonald-Kreitman framework in Table S6, we used Gene Ontology term assignments and resampling (using 10,000 resamples) as in Section 4.4, except that for P_n/P_s we tested for enrichment of low values of the metric across a given term. Genomic analyses on NI proceeded as above, except on the filtered dataset of genes with $P_n/P_s > a - 1.5\sigma$ as explained above and testing for enrichment of low values of the metric across the term. *p*-values were corrected for multiple testing by the Benjamini/Hochberg method using the multipletests function from statsmodels[82].

Acknowledgements

The authors thank Jamie Cate and Alexander Johnson for strains, and Johnson Jun-Ting Wang and members of the Brem lab for experimental support and helpful discussions. This work was supported by NIH 2R01GM120430 to R.B.B. and an NSF Graduate Research Fellowship to A.D.

Table Captions

Table 1. McDonald-Kreitman hit genes. Each row reports a gene with evidence for adaptive protein variation between *K. marxianus* and *K. lactis* according to the McDonald-Kreitman test (adjusted $p < 0.05$). NI, neutrality index. Genes highlighted in green also showed significant evidence for positive selection on the branch leading to *K. marxianus* in phylogenetic tests (PAML branch-site $p < 0.05$; Table S4). Not shown here are genes with p-value < 0.05 as a product of exceptionally high or low amino acid polymorphism; see Methods and Table S5.

Figure Captions

Figure 1. *K. marxianus* shows a unique heat and chemical stress resistance phenotype. A, Phylogenetic tree of the *Kluyveromyces* genus with marine and terrestrial species delineated[7,85]. Branch lengths are not to scale. **B,** Each panel reports the results of a growth profiling experiment across the genus in the indicated condition. In a given panel, each trace reports a growth timecourse for the indicated species, with the solid line displaying the mean across technical replicates and the faint outline showing the standard error. OD, optical density.

Figure 2. The unique heat tolerance of *K. marxianus* only manifests during its growing stage. A, Experimental workflow created with BioRender.com. From left, inoculum from a starting liquid culture is introduced into fresh liquid medium for regrowth at 28°C and then sampled at nutrient exhaustion (Stationary) or in log phase (Exponential). The liquid sample is subjected to a heat shock of 47°C for 30 minutes and then spotted as serial dilutions onto solid medium. Viable cells after heat shock grow into colonies after incubation at 28°C. **B**-**C**, Each row reports viability after heat shock of a sample of the indicated species in the indicated liquid growth phase. See Figure S3 for unshocked controls.

Figure 3. Overall regulatory volatility by *K. lactis* relative to *K. marxianus* and stress-evoked repression of glycolysis in both species. A, Shown are results of principal component (PC) analysis of *K. lactis* and *K. marxianus* transcriptomes across treatments. Each point reports the values of the top two PCs for one replicate transcriptome of the indicated species subjected to the indicated stress treatment or a 28°C unstressed control. In a given axis label, the value in parentheses reports the proportion of variance across the set of transcriptomes explained by the indicated PC. **B,C,** Each panel reports the effect of stress on expression of genes of the indicated Gene Ontology term in *K. marxianus* and *K. lactis*. In a given panel, each cell reports, for the indicated gene, the $\log_2$ fold-change between expression levels in the indicated stress treatment and an unstressed control.

Figure 4. Genetic or culture-based block of respiration compromises stress tolerance in *K. marxianus* and *K. lactis*. A, B, Each panel reports cell viability assays after culture in liquid medium with stress, or an unstressed control, of *K. marxianus* or *K. lactis* in normoxia or hypoxia. In a given panel, each row shows serial dilutions of the liquid culture spotted onto solid medium and incubated without stress at 28°C. **C,** Data are as in **A,B** except that panels report wild-type *K. marxianus* or an isogenic strain lacking the respiration factor *COX15*.

Figure 5. *K. marxianus* has many genes with independently evolving sites. A, Each bar shows the number of genes with significant evidence for positive selection on the indicated lineage (adjusted $p > 0.05$) in a phylogenetic PAML branch-site test. **B,** The set of bars of each color reports the distribution, across the genes from **A**, of the number of sites per gene inferred by PAML to be targets of positive selection on the indicated lineage. **C,** Amino acid alignment of an example region of a gene, KLLA0B02607g (*S. cerevisiae* ortholog FAT3/*YKL187C*), with evidence for positive selection from the PAML test in **A** and from the McDonald-Kreitman test of Table 1. Highlighted columns show inferred targets of positive selection from the PAML test in

B. Highlighting indicates the amino acid's BLOSUM 62 matrix score with respect to the consensus amino acid.

Supplementary Figure Captions

Figure S1. Stresses in which *K. marxianus* does not exhibit unique stress tolerance relative to the rest of the genus. Data and symbols are as in Figure 1B of the main text except that each panel reports growth measurements in the indicated stress.

Figure S2. *K. marxianus* strains mirror each other in heat tolerance. Data and symbols are as in Figure 1B of the main text except that in a given panel, each trace reports growth measurements of the indicated wild *K. marxianus* strain.

Figure S3. No detectable difference between *Kluyveromyces* species with respect to cell viability from unstressed liquid cultures. Data and symbols are as in Figure 2 of the main text except that liquid cultures were not subjected to heat shock before plating.

Figure S4. Stress-evoked changes in *K. lactis*, but not *K. marxianus,* dominate transcriptome comparisons between the two. A, Shown are results from the principal component (PC) analysis of *K. lactis* and *K. marxianus* transcriptomes across treatments in Figure 3A of the main text. Each panel reports expression across genotypes and treatments of the three genes contributing most to the indicated PC. In a given panel, each bar reports expression, as a mean across replicates, of the indicated gene in the indicated species and treatment. The full set of gene weights is listed in Supplementary Table 2. **B, C**, Data are as in Figure 3B,C of the main text except that genes of the indicated Gene Ontology term are reported.

Figure S5. Stress resistance of a *K. lactis* x *K. marxianus* hybrid is intermediate between that of the purebred parents. Data are as in Figure 1B of the main text except that each panel reports growth measurements of *K. lactis*, *K. marxianus*, and a *K. lactis* x *K. marxianus* F1 hybrid.

Supplementary Table Captions

Table S1. Strain table. List of strains used for phenotypic assays and population analyses. All species shown are haploid.

Table S2. Normalized RNA-seq read counts, major principal component weights, and stress effects. Each row reports RNA-seq results and analysis for a pair of orthologous *K. lactis* and *K. marxianus* genes. Columns B and C report respective weighting of the gene in the first and second components of a principal component analysis. In columns D-S, each column reports normalized RNA-seq read counts as an average across replicates from cultures of *K. lactis* or *K. marxianus* in unstressed control conditions (LC and MC, respectively) or in stress treatments (LT or MT, respectively), where stresses are 39°C, ethanol (ET), MMS, or caffeine (CAF). The last eight columns report the effect of stress on expression; each reports the average across replicates of $\log_2$(treatment/control) for each species in the indicated treatment.

Table S3. Gene Ontology terms with stress-responsive expression. Each tab reports the results of tests of Gene Ontology terms for enrichment of expression change between the indicated stress and unstressed controls in the indicated species. In a given tab, each row reports results for the indicated Gene Ontology term: the average, across genes and replicates, of $\log_2$(treatment/control), and the multiple testing-corrected significance of the enrichment for high magnitude of this value relative to a resampling null.

Table S4. Phylogenetic tests for evidence of positive selection. In a given row, columns C-I report the results of PAML branch-site tests package for positive selection in *K. marxianus* on the indicated orthogroup (see Table S7 for full orthogroup membership). Columns C-D report the significance of the improvement in fit to an alternative model stipulating positive selection relative to a null without positive selection, as a nominal *p*-value and after adjustment for multiple testing. Columns E and G report the number and proportion, respectively, of sites inferred to be under positive selection in the alternative model. Column F reports the average conservation of the latter across *K. marxianus* population isolates from Supplementary Data 2. Columns H and I report inferred protein evolutionary rates for the branch leading to *K. marxianus* (foreground) and for all other branches of the tree (background), respectively. Columns J-O report the analogous results from tests for positive selection in *K. lactis*. Columns P-Q list the gene name and function for the *S. cerevisiae* ortholog. Green highlighted cells indicate cases of $p < 0.05$.

Table S5. McDonald-Kreitman tests for evidence of positive selection. Each row reports results from a McDonald-Kreitman test on the indicated pair of orthologous genes between *K. lactis* and *K. marxianus*. D_s, number of divergent synonymous changes between species; D_n, number of divergent non-synonymous changes between species; P_s, number of polymorphic synonymous changes within species; P_n, number of polymorphic non-synonymous changes within species; NI, neutrality index (see Methods); *p* and *p*-value, nominal and multiple testing-corrected McDonald-Kreitman significances, respectively. Columns L-M list the gene name and function for the *S. cerevisiae* ortholog. Green highlighted cells indicate cases of $p < 0.05$.

Table S6. Gene Ontology terms with evidence for positive or purifying selection. Each tab reports the results of tests of Gene Ontology terms for enrichment of extreme values of one sequence-based metric of selection. These tests used the gene-based variation data from Table S5 and were, respectively, for low values of the neutrality index, NI, indicative of positive selection; for low values of P_s/P_n, indicative of purifying selection; and for high values of the protein evolutionary rate D_s/D_n, indicative of positive selection. In a given tab, each row reports results for the indicated Gene Ontology term: the average across genes of the indicated metric, and the nominal and the multiple testing-corrected significance of the enrichment for extreme magnitude of this value relative to a resampling null (p-value and p_adj, respectively).

Table S7. Orthologs across the *Kluyveromyces* genus used as input to PAML. Each row reports the genes of the indicated species representing the members of one inferred orthogroup.

Supplementary Data

Supplementary Data 1. Pseudogenomes and annotations.

Supplementary Data 2. Variant calls from population genomic resequencing.

References

1. Smith, S. D., Pennell, M. W., Dunn, C. W. & Edwards, S. V. Phylogenetics is the New Genetics (for Most of Biodiversity). *Trends in Ecology & Evolution* **35**, 415–425 (2020).
2. Weiss, C. V. & Brem, R. B. Dissecting Trait Variation across Species Barriers. *Trends in Ecology & Evolution* **34**, 1131–1136 (2019).
3. Masly, J. P. & Azom, M. G. Molecular divergence with major morphological consequences: development and evolution of organ size and shape. *Essays in Biochemistry* **66**, 707–716 (2022).
4. Shen, X.-X. *et al.* Tempo and Mode of Genome Evolution in the Budding Yeast Subphylum. *Cell* **175**, 1533-1545.e20 (2018).
5. Kurtzman, C., Fell, J. W. & Boekhout, T. *The Yeasts: A Taxonomic Study*. (Elsevier, 2011).
6. Nespolo, R. F. *et al.* Performance, genomic rearrangements, and signatures of adaptive evolution: Lessons from fermentative yeasts. *Ecology and Evolution* **10**, 5240–5250 (2020).
7. Varela, J. A. *et al.* Origin of Lactose Fermentation in Kluyveromyces lactis by Interspecies Transfer of a Neo-functionalized Gene Cluster during Domestication. *Current Biology* **29**, 4284-4290.e2 (2019).
8. Madeira-Jr, J. V. & Gombert, A. K. Towards high-temperature fuel ethanol production using Kluyveromyces marxianus: On the search for plug-in strains for the Brazilian sugarcane-based biorefinery. *Biomass and Bioenergy* **119**, 217–228 (2018).
9. Hoshida, H., Kagawa, S., Ogami, K. & Akada, R. Anoxia-induced mitophagy in the yeast Kluyveromyces marxianus. *FEMS Yeast Research* **20**, foaa057 (2020).
10. Lertwattanasakul, N. *et al.* Essentiality of respiratory activity for pentose utilization in thermotolerant yeast Kluyveromyces marxianus DMKU 3-1042. *Antonie van Leeuwenhoek* **103**, 933–945 (2013).

11. Kosaka, T. *et al.* Distinct Metabolic Flow in Response to Temperature in Thermotolerant Kluyveromyces marxianus. *Applied and Environmental Microbiology* **88**, e02006-21 (2022).

12. Mejía-Barajas, J. A. *et al.* Electron transport chain in a thermotolerant yeast. *J Bioenerg Biomembr* **49**, 195–203 (2017).

13. Wu, D., Wang, D. & Hong, J. Effect of a Novel Alpha/Beta Hydrolase Domain Protein on Tolerance of K. marxianus to Lignocellulosic Biomass Derived Inhibitors. *Frontiers in Bioengineering and Biotechnology* **8**, (2020).

14. Fu, X., Li, P., Zhang, L. & Li, S. Understanding the stress responses of Kluyveromyces marxianus after an arrest during high-temperature ethanol fermentation based on integration of RNA-Seq and metabolite data. *Appl Microbiol Biotechnol* **103**, 2715–2729 (2019).

15. Lane, M. M. *et al.* Physiological and metabolic diversity in the yeast Kluyveromyces marxianus. *Antonie van Leeuwenhoek* **100**, 507–519 (2011).

16. Cernak, P. *et al.* Engineering Kluyveromyces marxianus as a Robust Synthetic Biology Platform Host. *mBio* **9**, 10.1128/mbio.01410-18 (2018).

17. Sorrells, T. R., Booth, L. N., Tuch, B. B. & Johnson, A. D. Intersecting transcription networks constrain gene regulatory evolution. *Nature* **523**, 361–365 (2015).

18. Suzuki, T., Hoshino, T. & Matsushika, A. Draft Genome Sequence of Kluyveromyces marxianus Strain DMB1, Isolated from Sugarcane Bagasse Hydrolysate. *Genome Announcements* **2**, 10.1128/genomea.00733-14 (2014).

19. Avchar, R., Lanjekar, V., Dhakephalkar, P. K., Dagar, S. S. & Baghela, A. Compost as an untapped niche for thermotolerant yeasts capable of high□temperature ethanol production. *Letters in Applied Microbiology* **74**, 109–121 (2022).

20. Verma, S. *et al.* Influence of biochar on succession of fungal communities during food waste composting. *Bioresource Technology* **385**, 129437 (2023).

21. Yang, Z. PAML 4: Phylogenetic Analysis by Maximum Likelihood. *Molecular Biology and Evolution* **24**, 1586–1591 (2007).

22. Friedrich, A. *et al.* Contrasting Genomic Evolution Between Domesticated and Wild Kluyveromyces lactis Yeast Populations. *Genome Biology and Evolution* **15**, evad004 (2023).

23. McDonald, J. H. & Kreitman, M. Adaptive protein evolution at the Adh locus in Drosophila. *Nature* **351**, 652–654 (1991).

24. Lane, M. M. & Morrissey, J. P. Kluyveromyces marxianus: A yeast emerging from its sister's shadow. *Fungal Biology Reviews* **24**, 17–26 (2010).

25. Lappe-Oliveras, P. *et al.* Genotypic and Phenotypic Diversity of Kluyveromyces marxianus Isolates Obtained from the Elaboration Process of Two Traditional Mexican Alcoholic Beverages Derived from Agave: Pulque and Henequen (Agave fourcroydes) Mezcal. *Journal of Fungi* **9**, 795 (2023).

26. Naumov, G. I. Why Does the Yeast Kluyveromyces wickerhamii Assimilates but not Ferments Lactose? *Dokl Biol Sci* **403**, 310–312 (2005).

27. Ishtar Snoek, I. S. & Yde Steensma, H. Why does Kluyveromyces lactis not grow under anaerobic conditions? Comparison of essential anaerobic genes of Saccharomyces cerevisiae with the Kluyveromyces lactis genome. *FEMS Yeast Research* **6**, 393–403 (2006).

28. Nagahama, T., Hamamoto, M., Nakase, T. & Horikoshi, K. Kluyveromyces nonfermentans sp. nov., a new yeast species isolated from the deep sea. *International Journal of Systematic and Evolutionary Microbiology* **49**, 1899–1905 (1999).

29. Merico, A., Sulo, P., Piškur, J. & Compagno, C. Fermentative lifestyle in yeasts belonging to the Saccharomyces complex. *The FEBS Journal* **274**, 976–989 (2007).

30. Hagman, A., Säll, T., Compagno, C. & Piskur, J. Yeast "Make-Accumulate-Consume" Life Strategy Evolved as a Multi-Step Process That Predates the Whole Genome Duplication. *PLOS ONE* **8**, e68734 (2013).

31. Chikina, M., Robinson, J. D. & Clark, N. L. Hundreds of Genes Experienced Convergent Shifts in Selective Pressure in Marine Mammals. *Molecular Biology and Evolution* **33**, 2182–2192 (2016).

32. Castoe, T. A. *et al.* The Burmese python genome reveals the molecular basis for extreme adaptation in snakes. *Proceedings of the National Academy of Sciences* **110**, 20645–20650 (2013).

33. Pease, J. B., Haak, D. C., Hahn, M. W. & Moyle, L. C. Phylogenomics Reveals Three Sources of Adaptive Variation during a Rapid Radiation. *PLOS Biology* **14**, e1002379 (2016).

34. Kolora, S. R. R. *et al.* Origins and evolution of extreme life span in Pacific Ocean rockfishes. *Science* **374**, 842–847 (2021).

35. Woodard, S. H. *et al.* Genes involved in convergent evolution of eusociality in bees. *Proceedings of the National Academy of Sciences* **108**, 7472–7477 (2011).

36. Prado, M. R. *et al.* Milk kefir: composition, microbial cultures, biological activities, and related products. *Frontiers in Microbiology* **6**, (2015).

37. Gethins, L. *et al.* Acquisition of the yeast Kluyveromyces marxianus from unpasteurised milk by a kefir grain enhances kefir quality. *FEMS Microbiology Letters* **363**, fnw165 (2016).

38. Yazdi, M., Pahlevanlo, A. & Jamab, M. S. Diversity of Yeasts Microbiota in Iranian Doogh and Influence of Kluyveromyces Marxianus on its Protein profiles. *Applied Food Biotechnology* **9**, 41–52 (2022).

39. Ortiz-Merino, R. A. *et al.* Ploidy Variation in Kluyveromyces marxianus Separates Dairy and Non-dairy Isolates. *Frontiers in Genetics* **9**, (2018).

40. Williams, D. L., Schückel, J., Vivier, M. A., Buffetto, F. & Zietsman, A. J. J. Grape pomace fermentation and cell wall degradation by Kluyveromyces marxianus Y885. *Biochemical Engineering Journal* **150**, 107282 (2019).

41. Al-Qaysi, S. A. S., Abdullah, N. M., Jaffer, M. R. & Abbas, Z. A. Biological Control of Phytopathogenic Fungi by Kluyveromyces marxianus and Torulaspora delbrueckii Isolated from Iraqi Date Vinegar. *J Pure Appl Microbiol.* **15**, 300–311 (2021).

42. Spurley, W. J. *et al.* Substrate, temperature, and geographical patterns among nearly 2000 natural yeast isolates. *Yeast* **39**, 55–68 (2022).

43. Baptista, M., Cunha, J. T. & Domingues, L. Establishment of Kluyveromyces marxianus as a Microbial Cell Factory for Lignocellulosic Processes: Production of High Value Furan Derivatives. *Journal of Fungi* **7**, 1047 (2021).

44. Chacón-Vargas, K., Torres, J., Giles-Gómez, M., Escalante, A. & Gibbons, J. G. Genomic profiling of bacterial and fungal communities and their predictive functionality during pulque fermentation by whole-genome shotgun sequencing. *Sci Rep* **10**, 15115 (2020).

45. Anderson, P. J., McNeil, K. & Watson, K. High-Efficiency Carbohydrate Fermentation to Ethanol at Temperatures above 40°C by Kluyveromyces marxianus var. marxianus Isolated from Sugar Mills. *Applied and Environmental Microbiology* **51**, 1314–1320 (1986).

46. Baptista, M. & Domingues, L. Kluyveromyces marxianus as a microbial cell factory for lignocellulosic biomass valorisation. *Biotechnology Advances* **60**, 108027 (2022).

47. Burton, W. G. *Post-harvest Physiology of Food Crops*. (Longman, 1982).

48. Goodspeed, D. *et al.* Postharvest Circadian Entrainment Enhances Crop Pest Resistance and Phytochemical Cycling. *Current Biology* **23**, 1235–1241 (2013).

49. Rainey, T. J. & Covey, G. Pulp and paper production from sugarcane bagasse. in *Sugarcane-Based Biofuels and Bioproducts* 259–280 (John Wiley & Sons, Ltd, 2016). doi:10.1002/9781118719862.ch10.

50. Rij, N. J. W. K. *The Yeasts: A Taxonomic Study*. (Elsevier, 2013).

51. Hamad, I. *et al.* Culturomics and Amplicon-based Metagenomic Approaches for the Study of Fungal Population in Human Gut Microbiota. *Sci Rep* **7**, 16788 (2017).

52. Zhang, L., Zhan, H., Xu, W., Yan, S. & Ng, S. C. The role of gut mycobiome in health and diseases. *Therap Adv Gastroenterol* **14**, 17562848211047130 (2021).

53. Weiss, C. V. *et al.* Genetic dissection of interspecific differences in yeast thermotolerance. *Nat Genet* **50**, 1501–1504 (2018).

54. AlZaben, F., Chuong, J. N., Abrams, M. B. & Brem, R. B. Joint effects of genes underlying a temperature specialization tradeoff in yeast. *PLOS Genetics* **17**, e1009793 (2021).

55. Abrams, M. B. *et al.* Barcoded reciprocal hemizygosity analysis via sequencing illuminates the complex genetic basis of yeast thermotolerance. *G3 Genes|Genomes|Genetics* **12**, jkab412 (2022).

56. Boyle, E. A., Li, Y. I. & Pritchard, J. K. An Expanded View of Complex Traits: From Polygenic to Omnigenic. *Cell* **169**, 1177–1186 (2017).

57. Rockman, M. V. THE QTN PROGRAM AND THE ALLELES THAT MATTER FOR EVOLUTION: ALL THAT'S GOLD DOES NOT GLITTER. *Evolution* **66**, 1–17 (2012).

58. Montini, N. *et al.* Identification of a novel gene required for competitive growth at high temperature in the thermotolerant yeast Kluyveromyces marxianus. *Microbiology* **168**, 001148 (2022).

59. Hayward, L. K. & Sella, G. Polygenic adaptation after a sudden change in environment. *eLife* **11**, e66697 (2022).

60. Jain, K. & Stephan, W. Modes of Rapid Polygenic Adaptation. *Molecular Biology and Evolution* **34**, 3169–3175 (2017).

61. Bell, G. The Oligogenic View of Adaptation. *Cold Spring Harb Symp Quant Biol* **74**, 139–144 (2009).

62. Danecek, P. *et al.* Twelve years of SAMtools and BCFtools. *GigaScience* **10**, giab008 (2021).

63. Li, H. A statistical framework for SNP calling, mutation discovery, association mapping and population genetical parameter estimation from sequencing data. *Bioinformatics* **27**, 2987–2993 (2011).

64. Dujon, B. *et al.* Genome evolution in yeasts. *Nature* **430**, 35–44 (2004).

65. Emms, D. M. & Kelly, S. OrthoFinder: phylogenetic orthology inference for comparative genomics. *Genome Biology* **20**, 238 (2019).

66. Sorrells, T. R. *et al.* Intrinsic cooperativity potentiates parallel cis-regulatory evolution. *eLife* **7**, e37563 (2018).

67. Kim, D. *et al.* TopHat2: accurate alignment of transcriptomes in the presence of insertions, deletions and gene fusions. *Genome Biology* **14**, R36 (2013).

68. Anders, S., Pyl, P. T. & Huber, W. HTSeq—a Python framework to work with high-throughput sequencing data. *Bioinformatics* **31**, 166–169 (2015).

69. Robinson, M. D., McCarthy, D. J. & Smyth, G. K. edgeR: a Bioconductor package for differential expression analysis of digital gene expression data. *Bioinformatics* **26**, 139–140 (2010).

70. Pedregosa, F. *et al.* Scikit-learn: Machine Learning in Python. *Journal of Machine Learning Research* **12**, 2825–2830 (2011).

71. Kiers, J. *et al.* Regulation of alcoholic fermentation in batch and chemostat cultures of Kluyveromyces lactis CBS 2359. *Yeast* **14**, 459–469 (1998).

72. Dekker, W. J. C. *et al.* Engineering the thermotolerant industrial yeast Kluyveromyces marxianus for anaerobic growth. *Metabolic Engineering* **67**, 347–364 (2021).

73. Hsu, P.-C. *et al.* Plastic Rewiring of Sef1 Transcriptional Networks and the Potential of Nonfunctional Transcription Factor Binding in Facilitating Adaptive Evolution. *Molecular Biology and Evolution* **38**, 4732–4747 (2021).

74. Kluyveromyces nonfermentans genome assembly ASM3056991v1. *NCBI* https://www.ncbi.nlm.nih.gov/data-hub/assembly/GCA_030569915.1/.

75. Kluyveromyces aestuarii genome assembly ASM370755v2. *NCBI* https://www.ncbi.nlm.nih.gov/data-hub/assembly/GCA_003707555.2/.

76. Kluyveromyces dobzhanskii genome assembly ASM370580v3. *NCBI* https://www.ncbi.nlm.nih.gov/data-hub/assembly/GCA_003705805.3/.

77. Proux-Wéra, E., Armisén, D., Byrne, K. P. & Wolfe, K. H. A pipeline for automated annotation of yeast genome sequences by a conserved-synteny approach. *BMC Bioinformatics* **13**, 237 (2012).

78. Edgar, R. C. MUSCLE: multiple sequence alignment with high accuracy and high throughput. *Nucleic Acids Research* **32**, 1792–1797 (2004).

79. Suyama, M., Torrents, D. & Bork, P. PAL2NAL: robust conversion of protein sequence alignments into the corresponding codon alignments. *Nucleic Acids Research* **34**, W609–W612 (2006).

80. Zhang, J., Nielsen, R. & Yang, Z. Evaluation of an Improved Branch-Site Likelihood Method for Detecting Positive Selection at the Molecular Level. *Molecular Biology and Evolution* **22**, 2472–2479 (2005).

81. Yang, Z., Wong, W. S. W. & Nielsen, R. Bayes Empirical Bayes Inference of Amino Acid Sites Under Positive Selection. *Molecular Biology and Evolution* **22**, 1107–1118 (2005).

82. Seabold, S. & Perktold, J. Statsmodels: Econometric and Statistical Modeling with Python. in 92–96 (2010). doi:10.25080/Majora-92bf1922-011.

83. Cock, P. J. A. *et al.* Biopython: freely available Python tools for computational molecular biology and bioinformatics. *Bioinformatics* **25**, 1422–1423 (2009).

84. Li, H. Minimap2: pairwise alignment for nucleotide sequences. *Bioinformatics* **34**, 3094–3100 (2018).

85. Am-In, S., Yongmanitchai, W. & Limtong, S. Kluyveromyces siamensis sp. nov., an ascomycetous yeast isolated from water in a mangrove forest in Ranong Province, Thailand. *FEMS Yeast Research* **8**, 823–828 (2008).

Table 1.

K. lactis, K. marxianus genes	NI	*Saccharomyces* gene	Standard Name	Function
KLLA0E09329g, KM020H00950	0.19	YOR020W-A	MCO10	Subunit l of the mitochondrial F1F0 ATP synthase
KLLA0E07569g, KM020D04120	0.26	YKL060C	FBA1	Fructose 1,6-bisphosphate aldolase
KLLA0D10780g, KM020E01340	0.32	YJR118C	ILM1	Unknown function, possible mitochondrial involvement
KLLA0C12133g, KM020H02920	0.39	YNL284C	MRPL10	Mitochondrial ribosomal protein
KLLA0A10175g, KM020A03410	0.47	YMR313C	TGL3	Triacylglycerol lipase and LPE acyltransferase
KLLA0F19162g, KM020D01640	0.49	YDR111C	ALT2	Catalytically inactive alanine transaminase
KLLA0B04994g, KM020F01720	0.50	YLR443W	ECM7	Putative integral membrane protein, calcium uptake
KLLA0F00528g, KM020F00240	0.51	YAL061W	BDH2	Putative medium-chain alcohol dehydrogenase
KLLA0B02607g, KM020D05580	0.59	YKL187C	FAT3	Fatty acid uptake
KLLA0D16236g, KM020F04880	0.63	YGR130C	N/A	Component of the eisosome
KLLA0F26048g, KM020E04040	0.68	YMR066W	SOV1	Mitochondrial protein of unknown function

Figure 1

A

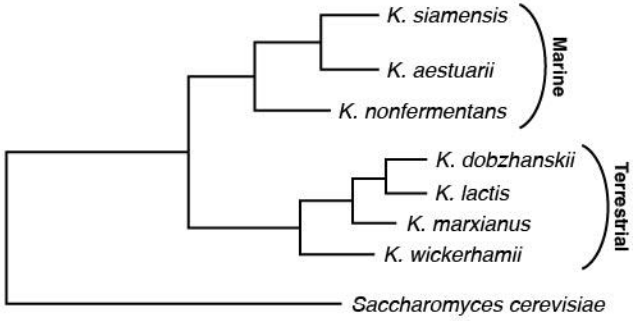
K. siamensis
K. aestuarii
K. nonfermentans
Marine
K. dobzhanskii
K. lactis
K. marxianus
K. wickerhamii
Terrestrial
Saccharomyces cerevisiae

B

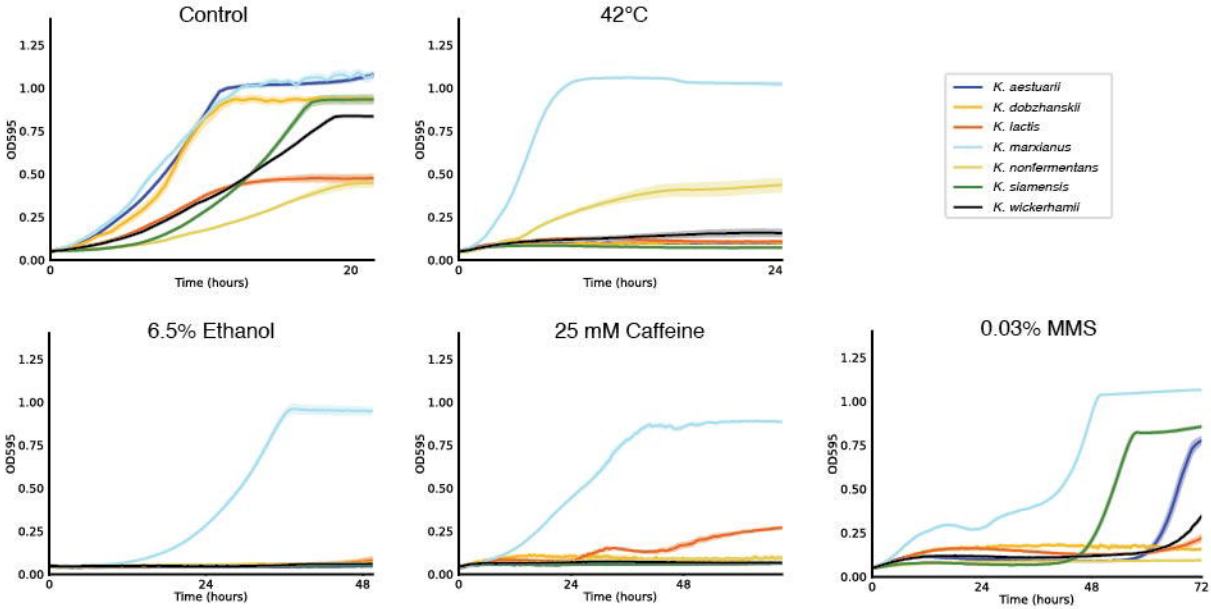
Control
42°C
6.5% Ethanol
25 mM Caffeine
0.03% MMS
OD595
Time (hours)
K. aestuarii
K. dobzhanskii
K. lactis
K. marxianus
K. nonfermentans
K. siamensis
K. wickerhamii

Figure 2

A

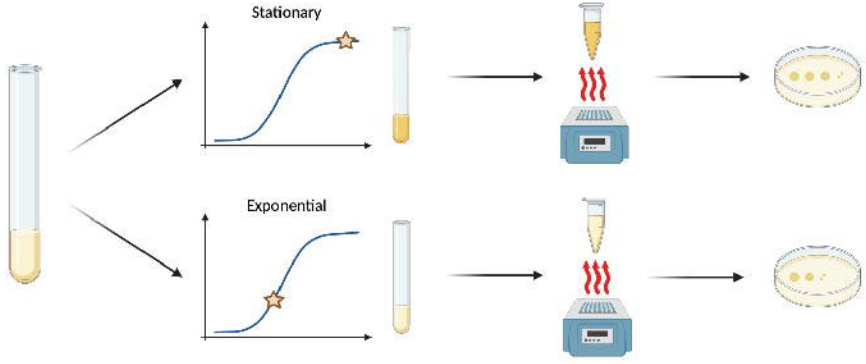
Stationary
Exponential

B

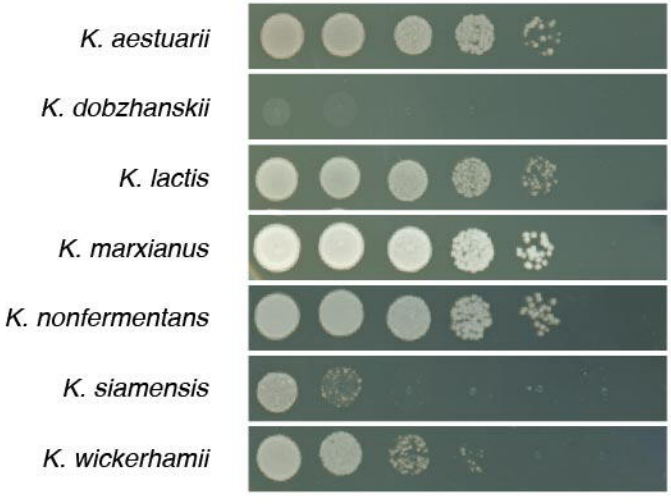
Stationary
K. aestuarii
K. dobzhanskii
K. lactis
K. marxianus
K. nonfermentans
K. siamensis
K. wickerhamii

C

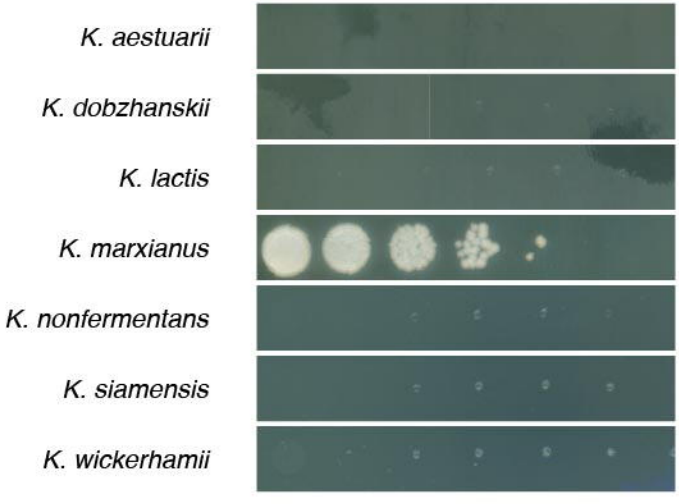
Exponential
K. aestuarii
K. dobzhanskii
K. lactis
K. marxianus
K. nonfermentans
K. siamensis
K. wickerhamii

Figure 3

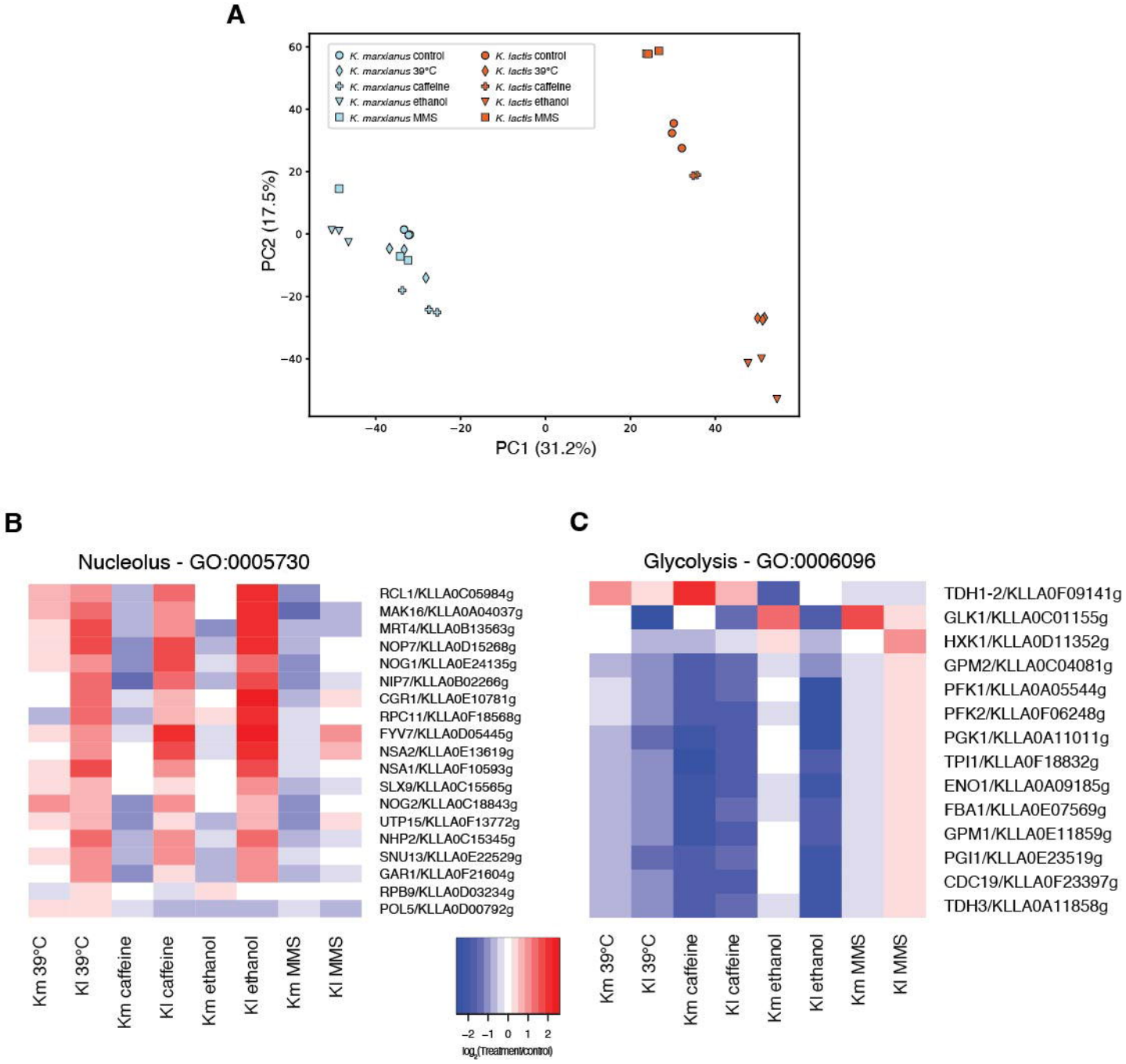
A
K. marxianus control
K. marxianus 39°C
K. marxianus caffeine
K. marxianus ethanol
K. marxianus MMS
K. lactis control
K. lactis 39°C
K. lactis caffeine
K. lactis ethanol
K. lactis MMS
PC2 (17.5%)
PC1 (31.2%)
B
Nucleolus - GO:0005730
RCL1/KLLA0C05984g
MAK16/KLLA0A04037g
MRT4/KLLA0B13563g
NOP7/KLLA0D15268g
NOG1/KLLA0E24135g
NIP7/KLLA0B02266g
CGR1/KLLA0E10781g
RPC11/KLLA0F18568g
FYV7/KLLA0D05445g
NSA2/KLLA0E13619g
NSA1/KLLA0F10593g
SLX9/KLLA0C15565g
NOG2/KLLA0C18843g
UTP15/KLLA0F13772g
NHP2/KLLA0C15345g
SNU13/KLLA0E22529g
GAR1/KLLA0F21604g
RPB9/KLLA0D03234g
POL5/KLLA0D00792g
Km 39°C
Kl 39°C
Km caffeine
Kl caffeine
Km ethanol
Kl ethanol
Km MMS
Kl MMS
log2(Treatment/control)
C
Glycolysis - GO:0006096
TDH1-2/KLLA0F09141g
GLK1/KLLA0C01155g
HXK1/KLLA0D11352g
GPM2/KLLA0C04081g
PFK1/KLLA0A05544g
PFK2/KLLA0F06248g
PGK1/KLLA0A11011g
TPI1/KLLA0F18832g
ENO1/KLLA0A09185g
FBA1/KLLA0E07569g
GPM1/KLLA0E11859g
PGI1/KLLA0E23519g
CDC19/KLLA0F23397g
TDH3/KLLA0A11858g
Km 39°C
Kl 39°C
Km caffeine
Kl caffeine
Km ethanol
Kl ethanol
Km MMS
Kl MMS

Figure 4

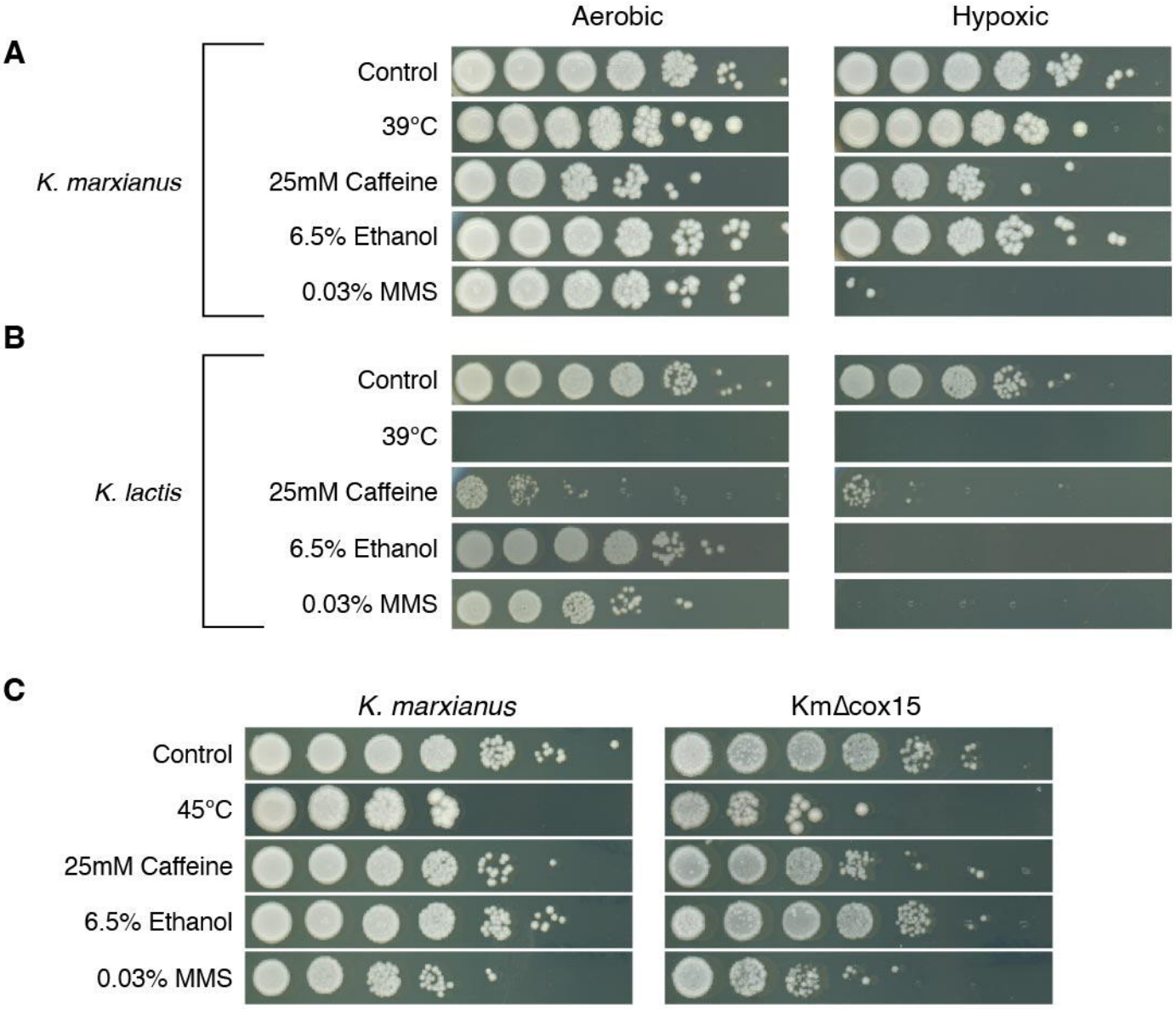
A
Aerobic
Hypoxic
K. marxianus
Control
39°C
25mM Caffeine
6.5% Ethanol
0.03% MMS
B
K. lactis
Control
39°C
25mM Caffeine
6.5% Ethanol
0.03% MMS
C
K. marxianus
KmΔcox15
Control
45°C
25mM Caffeine
6.5% Ethanol
0.03% MMS

Figure 5

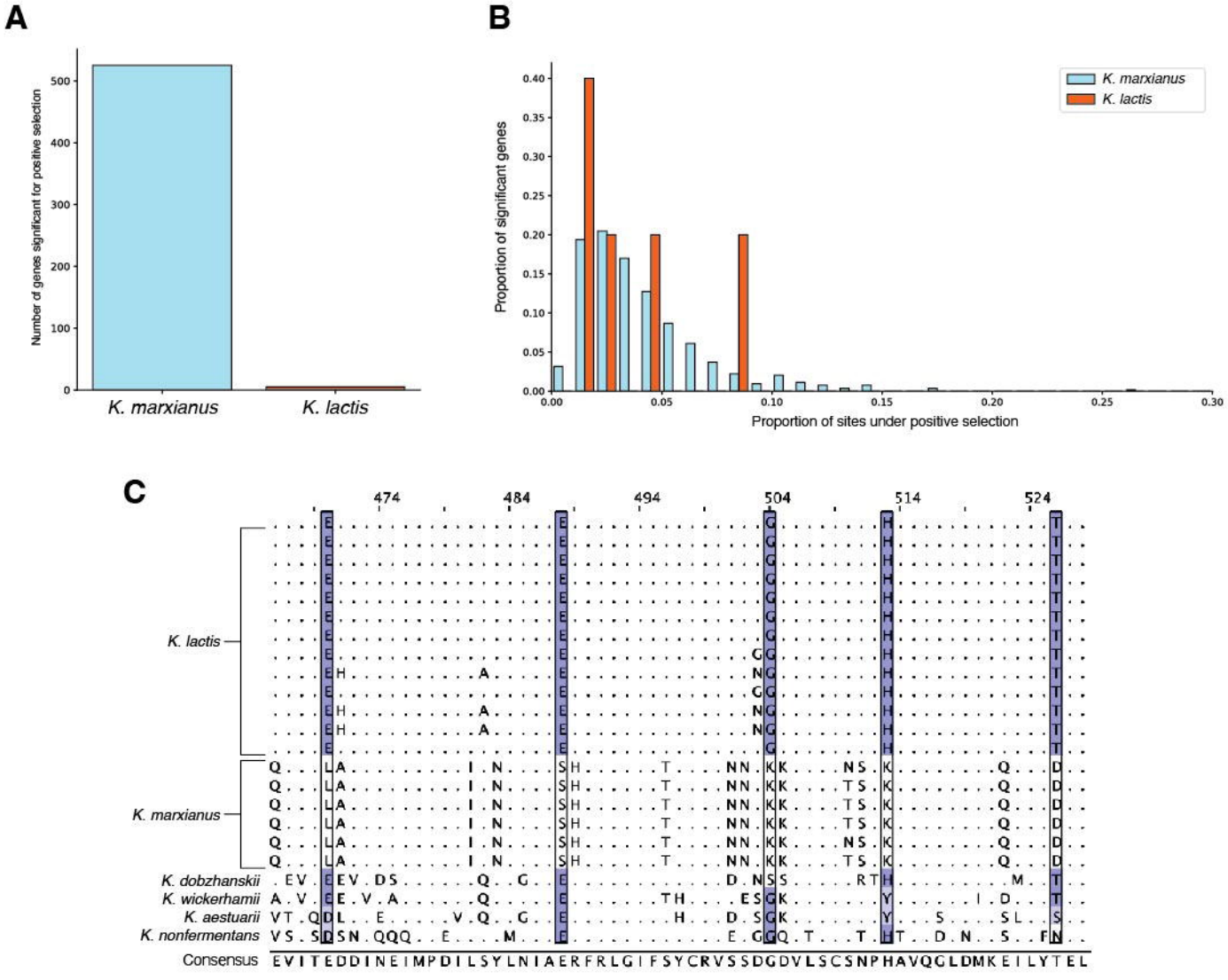
A
Number of genes significant for positive selection
0
100
200
300
400
500
K. marxianus
K. lactis
B
Proportion of significant genes
0.00
0.05
0.10
0.15
0.20
0.25
0.30
0.35
0.40
Proportion of sites under positive selection
0.00
0.05
0.10
0.15
0.20
0.25
0.30
K. marxianus
K. lactis
C
474
484
494
504
514
524
K. lactis
K. marxianus
K. dobzhanskii
K. wickerhamii
K. aestuarii
K. nonfermentans
Consensus
EVITEDDINEIMPDILSYLNIAERFRLGIFSYCRVSSDGDVLSCSNPHAVQGLDMKEILYTEL

Figure S1

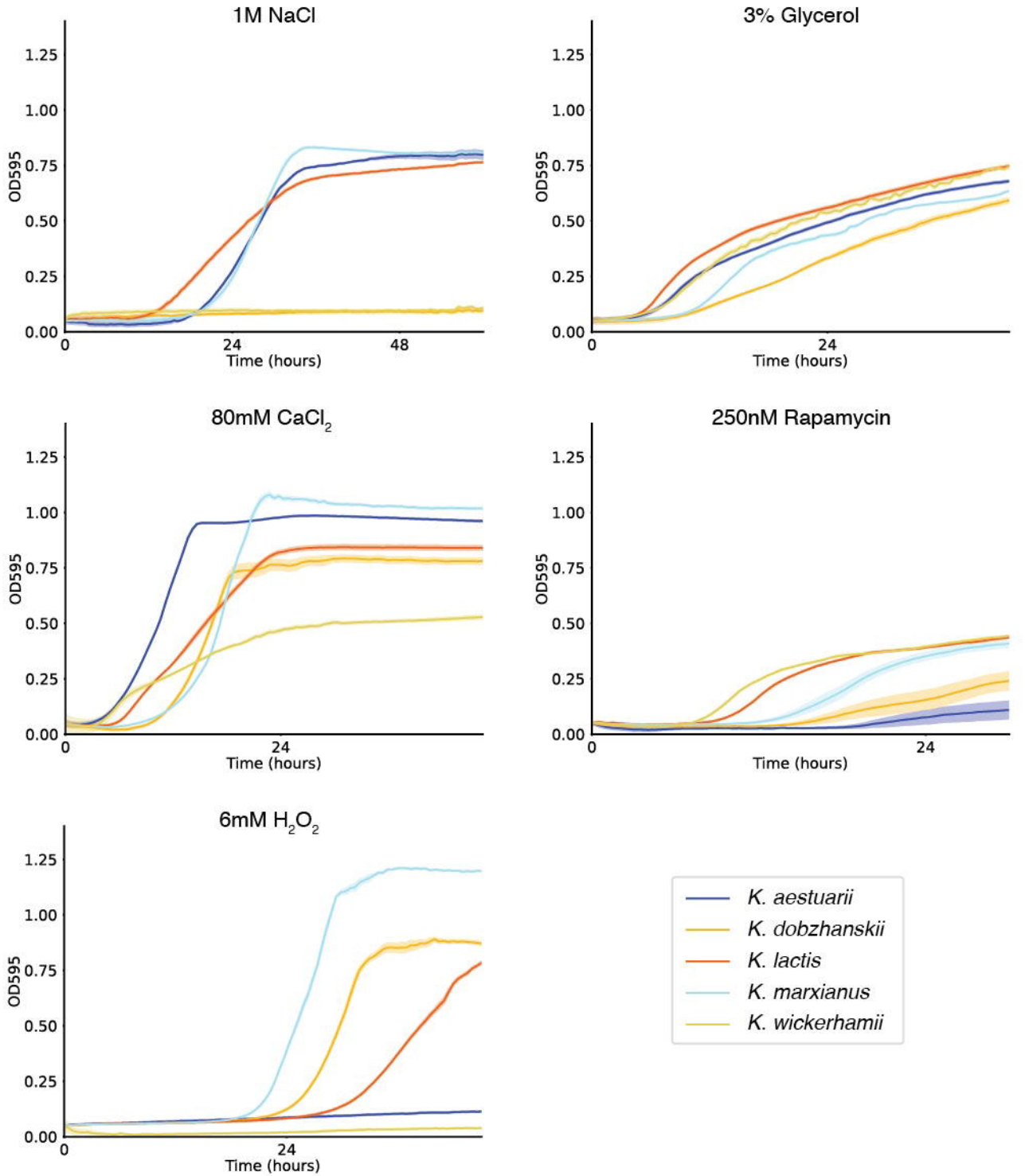
1M NaCl
3% Glycerol
80mM $CaCl_2$
250nM Rapamycin
6mM H_2O_2
OD595
Time (hours)
0.00
0.25
0.50
0.75
1.00
1.25
0
24
48
K. aestuarii
K. dobzhanskii
K. lactis
K. marxianus
K. wickerhamii

Figure S2

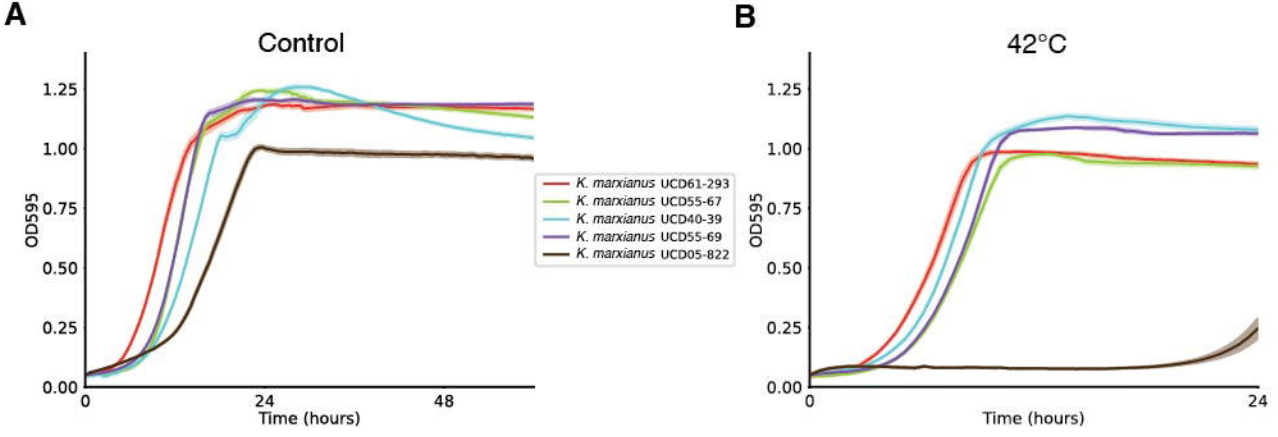
A
Control
1.25
1.00
0.75
0.50
0.25
0.00
OD595
0
24
48
Time (hours)
K. marxianus UCD61-293
K. marxianus UCD55-67
K. marxianus UCD40-39
K. marxianus UCD55-69
K. marxianus UCD05-822
B
42°C
1.25
1.00
0.75
0.50
0.25
0.00
OD595
0
24
Time (hours)

Figure S3

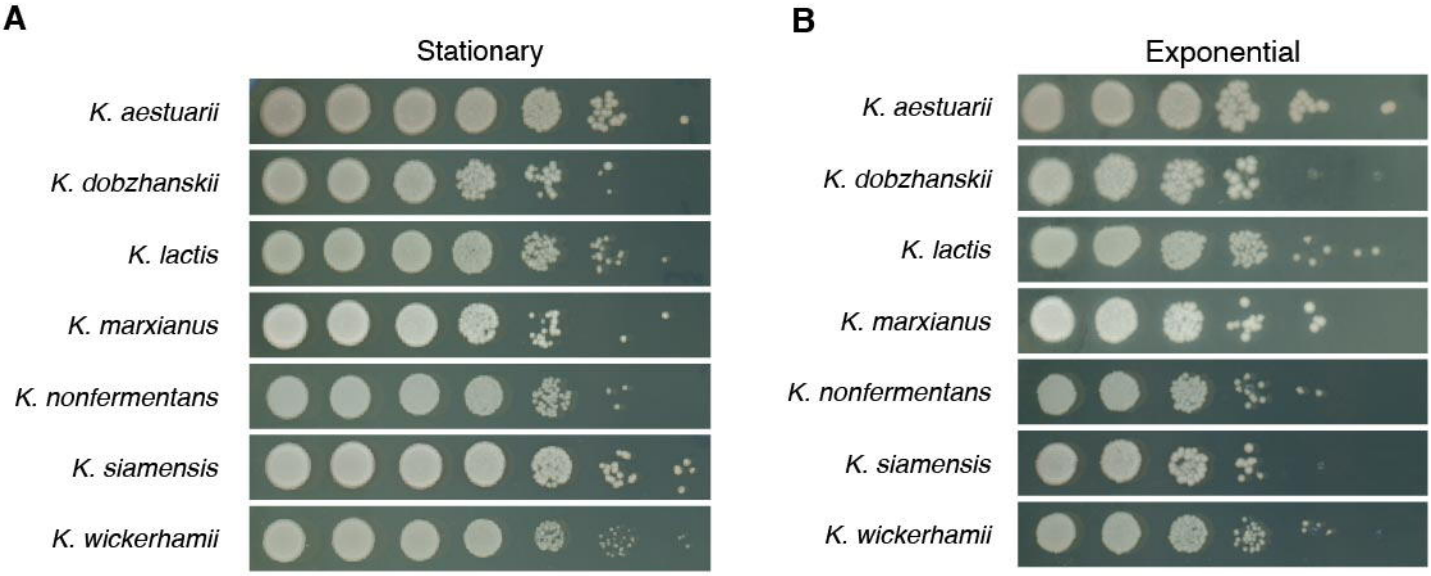
A
Stationary
K. aestuarii
K. dobzhanskii
K. lactis
K. marxianus
K. nonfermentans
K. siamensis
K. wickerhamii
B
Exponential
K. aestuarii
K. dobzhanskii
K. lactis
K. marxianus
K. nonfermentans
K. siamensis
K. wickerhamii

Figure S4

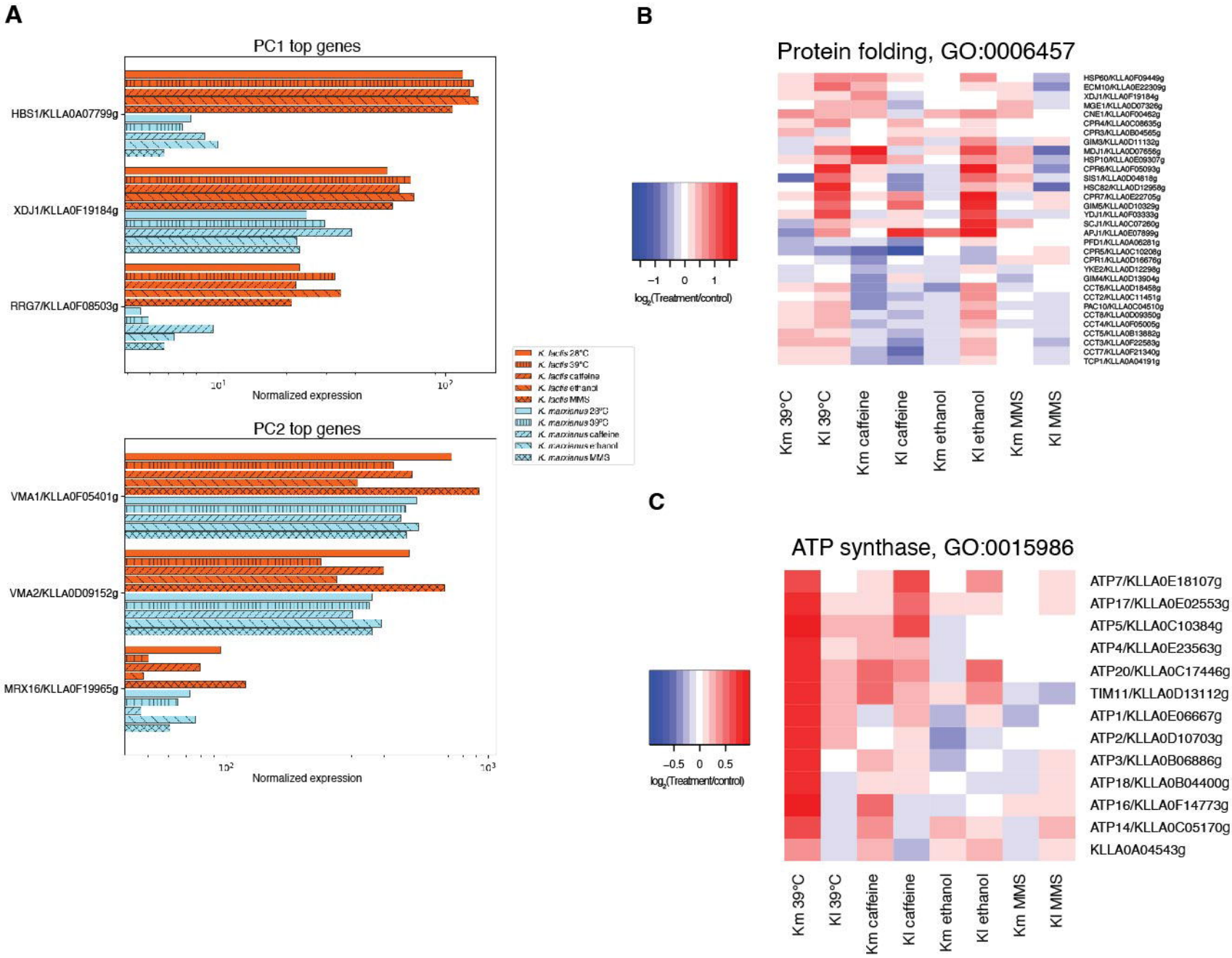
A
PC1 top genes
HBS1/KLLA0A07799g
XDJ1/KLLA0F19184g
RRG7/KLLA0F08503g
Normalized expression
PC2 top genes
VMA1/KLLA0F05401g
VMA2/KLLA0D09152g
MRX16/KLLA0F19965g
Normalized expression
K. lactis 28°C
K. lactis 39°C
K. lactis caffeine
K. lactis ethanol
K. lactis MMS
K. marxianus 28°C
K. marxianus 39°C
K. marxianus caffeine
K. marxianus ethanol
K. marxianus MMS
B
Protein folding, GO:0006457
log2(Treatment/control)
Km 39°C
Kl 39°C
Km caffeine
Kl caffeine
Km ethanol
Kl ethanol
Km MMS
Kl MMS
C
ATP synthase, GO:0015986
log2(Treatment/control)
ATP7/KLLA0E18107g
ATP17/KLLA0E02553g
ATP5/KLLA0C10384g
ATP4/KLLA0E23563g
ATP20/KLLA0C17446g
TIM11/KLLA0D13112g
ATP1/KLLA0E06667g
ATP2/KLLA0D10703g
ATP3/KLLA0B06886g
ATP18/KLLA0B04400g
ATP16/KLLA0F14773g
ATP14/KLLA0C05170g
KLLA0A04543g
Km 39°C
Kl 39°C
Km caffeine
Kl caffeine
Km ethanol
Kl ethanol
Km MMS
Kl MMS

Figure S5

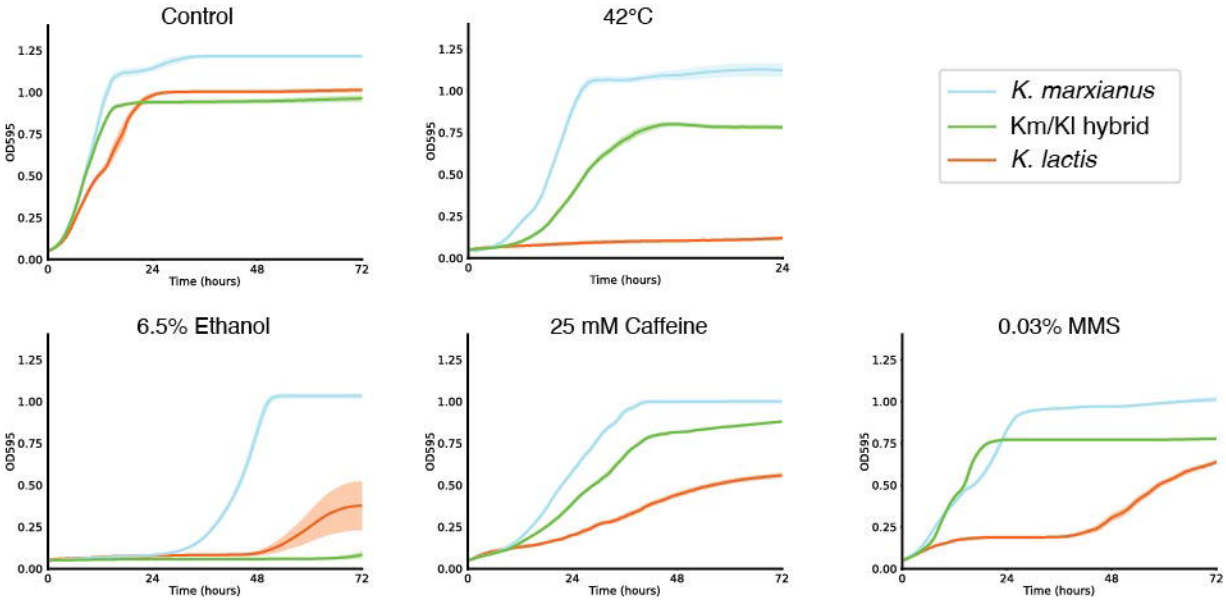
Control
42°C
6.5% Ethanol
25 mM Caffeine
0.03% MMS
OD595
Time (hours)
0.00
0.25
0.50
0.75
1.00
1.25
0
24
48
72
K. marxianus
Km/Kl hybrid
K. lactis